NOTICE

The quality of this microform is heavily dependent upon the quality of the original thesis submitted for microfilming. Every effort has been made to ensure the highest quality of reproduction possible.

If pages are missing, contact the university which granted the degree.

Some pages may have indistinct print especially if the original pages were typed with a poor typewriter ribbon or if the university sent us an inferior photocopy.

Previously copyrighted materials (journal articles, published tests, etc.) are not filmed.

Reproduction in full or in part of this microform is governed by the Canadian Copyright Act, R.S.C. 1970, c. C-30.

AVIS

La qualité de cette microforme dépend grandement de la qualité de la thèse soumise au microfilmage. Nous avons tout fait pour assurer une qualité supérieure de reproduction.

S'il manque des pages, veuillez communiquer avec l'université qui a conféré le grade.

La qualité d'impression de certaines pages peut laisser à désirer, surtout si les pages originales ont été dactylographiées à l'aide d'un ruban usé ou si l'université nous a fait parvenir une photocopie de qualité inférieure.

Les documents qui font déjà l'objet d'un droit d'auteur (articles de revue, tests publiés, etc.) ne sont pas microfilmés.

La reproduction, même partielle, de cette microforme est soumise à la Loi canadienne sur le droit d'auteur, SRC 1970, c. C-30.

Canadä

THE UNIVERSITY OF ALBERTA

The Effect of Argon-Freon Shielding Gas Mixtures on Gas Metal Arc
Welding of Aluminum

by

(C) Chunteak Choo

A THESIS

SUBMITTED TO THE FACULTY OF GRADUATE STUDIES AND

RESEARCH

IN PARTIAL FULFILMENT OF THE REQUIREMENTS FOR THE

DEGREE

OF Master of Science in Metallurgical Engineering

Department of Mining, Metallurgical and Petroleum Engineering

EDMONTON, ALBERTA

Fall 1988

Permission has been granted to the National Library of Canada to microfilm this thesis and to lend or sell copies of the film.

The author (copyright owner) has reserved other publication rights, and neither the thesis nor extensive extracts from it may be printed or otherwise reproduced without his/her written permission.

L'autorisation a été accordée à la Bibliothèque nationale du Canada de microfilmer cette thèse et de prêter ou de vendre des exemplaires du film.

L'auteur (titulaire du droit d'auteur) se réserve les autres droits de publication; ni la thèse ni de longs extraits de celle-ci ne doivent être imprimés ou autrement reproduits sans son autorisation écrite.

THE UNIVERSITY OF ALBERTA
RELEASE FORM

NAME OF AUTHOR   Chunteak Choo

TITLE OF THESIS   The Effect of Argon-Freon Shielding Gas Mixtures on Gas Metal Arc Welding of Aluminum

DEGREE FOR WHICH THESIS WAS PRESENTED   Master of Science

YEAR THIS DEGREE GRANTED   1988

Permission is hereby granted to THE UNIVERSITY OF ALBERTA LIBRARY to reproduce single copies of this thesis and to lend or sell such copies for private, scholarly or scientific research purposes only.

The author reserves other publication rights, and neither the thesis nor extensive extracts from it may be printed or otherwise reproduced without the author's written permission.

(SIGNED) ....

PERMANENT ADDRESS:

8616 - 22 Ave.

Edmonton, Alta.

T6K 1Z8

DATED ....July 22........ 1988

THE UNVERSITY OF ALBERTA

FACULTY OF GRADUATE STUDIES AND RESEARCH

The undersigned certify that they have read, and recommend to the Faculty of Graduate Studies and Research, for acceptance, a thesis entitled The Effect of Argon-Freon Shielding Gas Mixtures on Gas Metal Arc Welding of Aluminum submitted by Chunteak Choo in partial fulfilment of the requirements for the degree of Master of Science in Metallurgical Engineering.

....
Supervisor

....

....

....

Date ....July 22, 1988.......

Dedication

I dedicate this thesis to my parents and my wife.

Abstract

Attempts to improve arc stability and weld bead characteristics (e.g. penetration) for welding ferrous and non-ferrous alloys with the Gas Metal Arc Welding (GMAW) process have often involved modifications to the shielding gas. In this present work, three different shielding gas mixtures (pure argon, argon - 2% freon 12 (CCl_2F_2) and argon - 2% freon 11 (CCl_3F)) were studied using both electrode positive and electrode negative operation with 1.6mm diameter 5356 aluminum wire on 5086 aluminum plate.

Regardless of the shielding gas, a high droplet frequency spray transfer was observed on electrode positive, while a much lower transfer frequency (globular or gravity transfer) was observed on electrode negative because of the smaller current density gradient (i.e., the lower plasma jet velocity) caused by the lowering of heat input to the anode during electrode negative operation. This lower heat input to the anode caused a decrease in penetration and produced a poorer weld profile.

Comparing the three shielding gas mixtures, evaluation showed that an increased chlorine content in the shielding gas increased constriction of the arc column, and therefore decreased fusion width on both polarities. It was also found that arc stability and penetration improved due to an increasing plasma jet velocity as chlorine content increased, and arc length increased due to a lowering of the total electrode voltage drop. Although the current density gradient is decreased due to a long arc length using argon - 2% freon 11 gas mixture, the plasma jet velocity is increased considerably to give a higher droplet transfer frequency, and a higher velocity and acceleration of the droplet on both electrode polarities. This is

believed to occur because argon - 2% freon 11 gas has the better physical properties (i.e., a lower dynamic viscosity and higher density).

Acknowledgements

I would like to thank my supervisor, Dr. B.M. Patchett, for his encouragement and guidance throughout my research. My appreciation is also extended to the technical staff in the Department for their assistance, in particular, Mr. C. Bicknell and Mrs C. Barker.

I would also like to thank Mr. R. Hailey in the Department of Electrical Engineering for supplying the high speed video machine used in this project.

Table of Contents

ix

List of Tables

x

List of Figures

1. General Introduction

The Gas Metal Arc Welding (GMAW) process is widely used for welding aluminum and its alloys because it provides more efficient filling of a groove or joint than the gas tungsten arc welding (GTAW) process. As a result, using the appropriate shielding gas, electrode, and welding conditions the GMAW process is utilized particularly in high production welding operations. Normally the vast majority of GMAW applications requires the use of direct current (D.C.) electrode positive polarity to achieve a stable arc, smooth metal transfer, relatively low spatter loss, and good weld bead characteristics for the entire range of welding currents used. Even though D.C. electrode negative polarity gives higher electrode melting rate than D.C. electrode positive, D.C. electrode negative is seldom used because the arc becomes unstable and erratic, and penetration is lower than that of D.C. electrode positive.

Other than type and polarity of current, shielding gas composition is the most important variable that influences arc stability and weld bead characteristics (e.g. penetration). Although the primary purpose of the shielding gas in GMAW is to protect the molten weld metal from contamination and damage by the surrounding atmosphere, improved arc stability and better weld bead characteristics can be also obtained concurrently by mixing controlled quantities of reactive gases with an inert gas such as argon and helium. The common reactive gases include oxygen, nitrogen, and carbon dioxide. It is common practice in GMAW of ferrous alloys to add oxygen or oxygen-bearing gases such as carbon dioxide to an inert gas to create a shielding gas. The oxygen atoms affect arc stability favourably, resulting in improved metal transfer characteristics even on

electrode negative polarity[1]. However, oxygen additions cannot be used when welding aluminum because refractory oxides form both at the surface and in the interior of the weld and therefore inhibit proper metal transfer and deposition, and thus degrade the mechanical properties by creating flaws, incomplete penetration and porosity.

With this in mind, other oxidizing atoms such as chlorine have been used in the consumable electrode welding of aluminum. Chlorine, however, is difficult to handle, and causes operator illness because it is highly toxic. To avoid this problem, it has been suggested that non-toxic gases such as freons (containing carbon, fluorine, bromine, and chlorine) could be used to replace chlorine gas[2-5]. It has further been reported that freons containing higher numbers of chlorine atoms provided the most improvements in arc characteristics on both D.C. electrode polarities[6]. Two freons were chosen for experimentation purposes in this thesis project: freon 12 (CCl_2F_2) and freon 11 (CCl_3F).

The purpose of this project was to compare the effects of the various freon additions to argon with that of pure argon shielding gas on arc stability, metal transfer, and weld profile and appearance using both D.C. electrode polarities. Another goal of this project was to determine optimum welding conditions for both D.C. electrode polarities using an argon - 2% freon 11 shielding gas mixture and to evaluate the mechanical properties of the resulting weld metal deposits.

2. Literature Survey

2.1 Survey Introduction

The gas metal arc welding (GMAW) process is a method of welding in which an electric arc is maintained between a continuous filler metal (consumable) electrode and the work piece in a protected gas atmosphere. Shielding of the arc and molten weld pool is obtained entirely from an externally supplied gas or gas mixture.

When GMAW was first developed shortly after the gas tungsten arc welding process, it was originally introduced to industry as a rapid method for the fusion welding of aluminum and aluminum alloys using an inert gas for arc shielding. As a result, the term MIG (Metal Inert Gas) was used and is still the most common reference for the process. However, the users of this process turned to gases other than argon or helium such as CO_2 and O_2 (particularly for ferrous metals) and coined the term MAG (Metal Active Gas). Therefore, the designation "gas metal arc welding" (GMAW) was eventually adopted for the process. In addition to changes in the nature of the shielding gases employed, type and polarity of current, and power source design and performance have developed to permit its application to a broader range of materials.

Let us consider this process and attempt to picture what happens in the welding zone. First, the general physics of the arc is taken up from the experimental point of view. This is followed by sections dealing with the effect of welding speed on weld metal, arcs in various atmospheres, and the transfer of metal across the arc.

2.2   The Physics of the Arc

2.2.1   Voltage-Arc Length Characteristics

It is commonly assumed that the total arc voltage is made up of three separate and distinct parts the cathode potential drop, the potential drop in the arc column and the anode potential drop:

$$V = V_c + V_p + V_a \qquad (1)$$

A typical example is shown in Figure 1. There is a sharp drop of potential close to the electrodes and a gradual and approximately linear fall in the arc proper. It is customary to determine the plasma potential gradient from the slope of the voltage-arc length curve. The anode and cathode potential drops may reasonably be obtained by extrapolating this straight line (middle portion) to each end. In such measurements, the electrode potential drops are assumed to be independent of arc length. However, in high current welding arcs at atmospheric pressure and relatively short lengths this procedure may not be satisfactory, since the electrode drops depend on the electrode separation[7,8].

Olsen[9] illustrated the significance of the measured voltage-arc length characteristics for GMAW process as shown in Figure 2. The differences between the calculated plasma potential drops, obtained by integration of the field distributions calculated from measured temperatures, and the measured total arc potentials for different electrode separations are plotted as the sum of the cathode and anode potential drops. The downward trend of the measured total arc potential curve is shown to be caused by changes in the electrode potential drop with the electrode separation in short arcs.
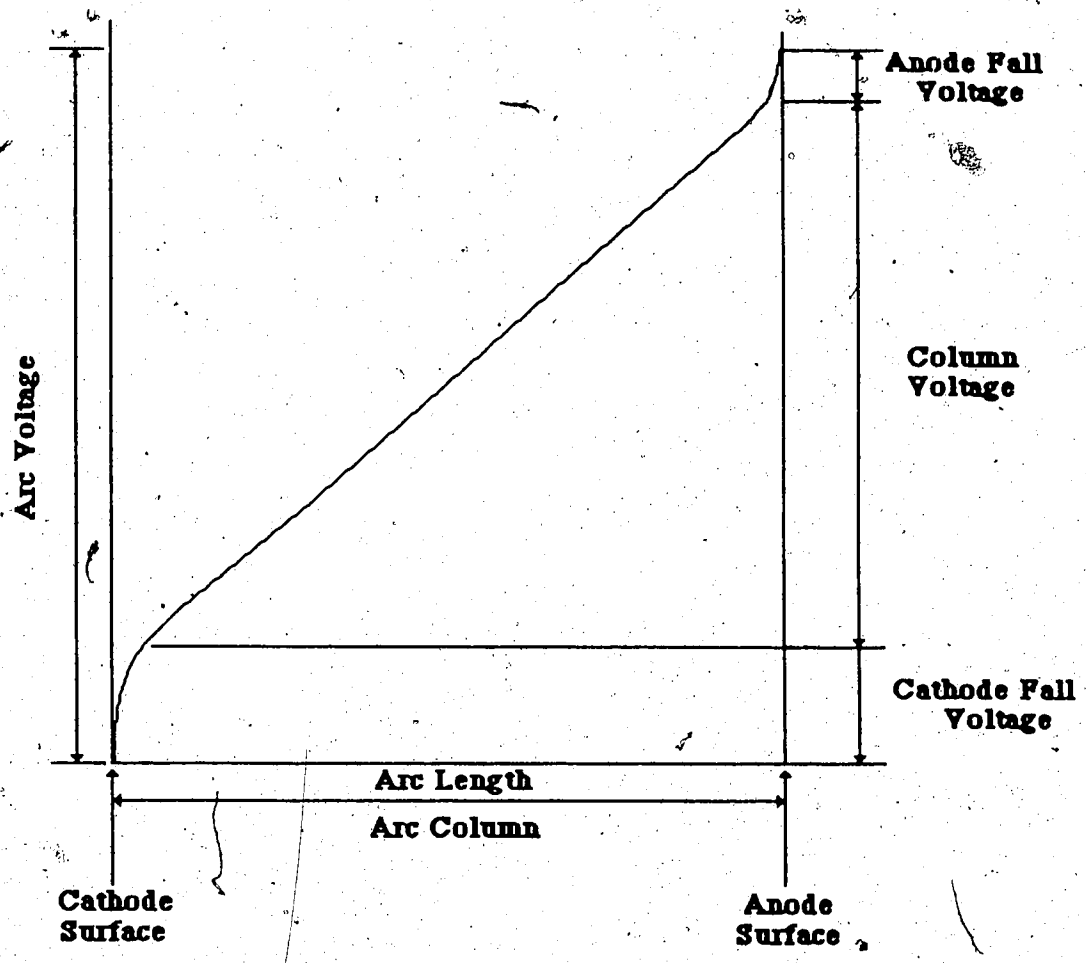
Figure 1. Voltage Distribution along an Arc shown diagrammatically
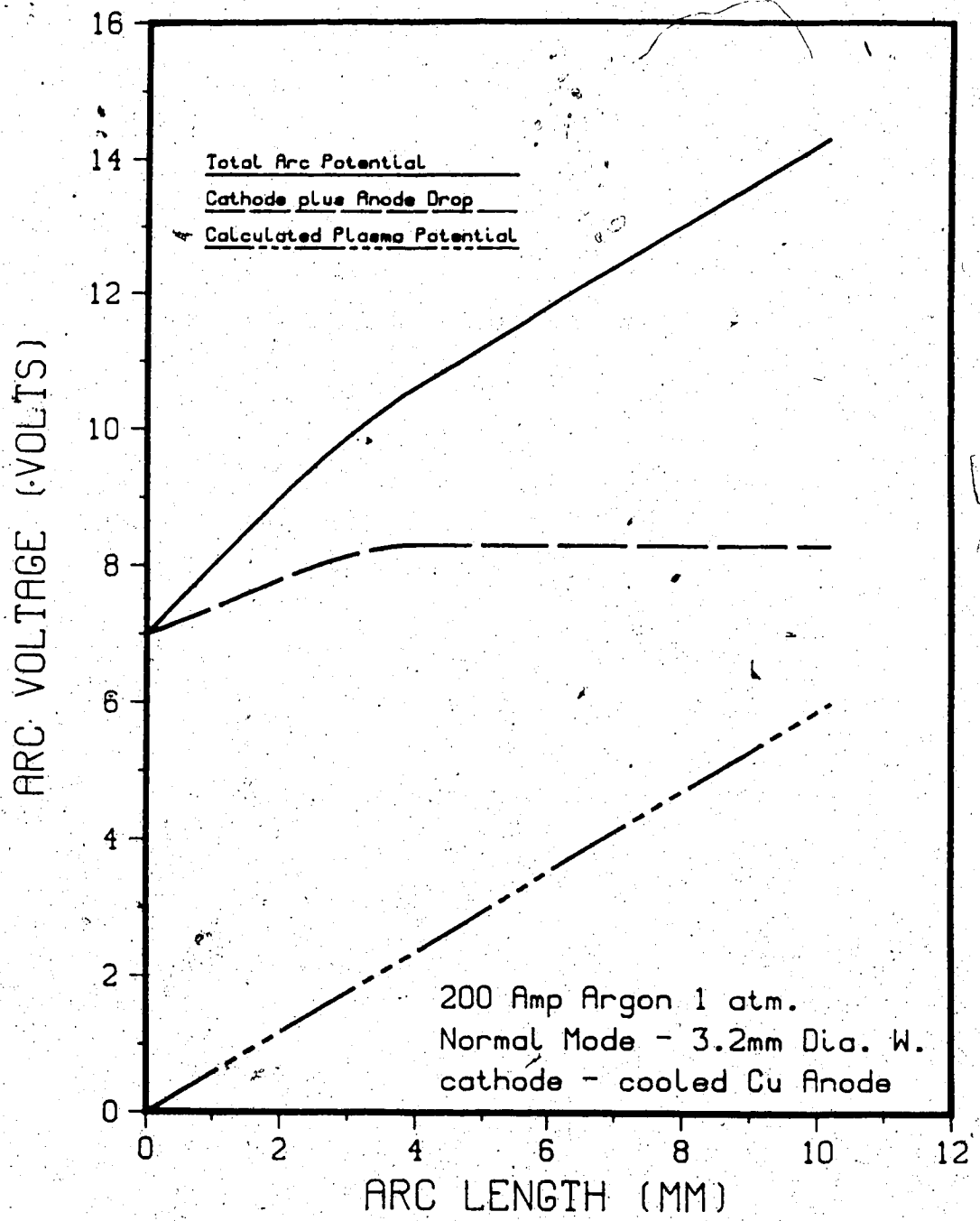
Figure 2. Comparison of Total Arc Potentials
and Plasma Potentials Calculated from
Measured Temperature Distributions
(modified from reference 9)

Extrapolation to zero length with constant slope from points at lengths greater than 4.0 mm gives a constant value for the long arc electrode potential drops.

A number of investigations[10-13] have studied the voltage-arc length characteristics for the consumable aluminum electrode arc welding processes at various welding currents. Results in Figure 3 show that as the welding current is decreased, the total arc potential at a given arc length and the sum of the anode and cathode potential drops obtained by extrapolating the curve to zero arc length, both decrease significantly. As expected, the downward trend of the curve was observed in shorter arc lengths as in the GTAW process. However, voltage gradients measured in the region of the arc in which the gradient remained constant were found to be about 0.63 volts/mm for any given welding current. The variations in the measured voltage gradients could be explained by the sensitivity of the voltage-ampere characteristics to slight changes in electrode material, geometry and to the mechanism of the cathode potential drop.

Muller et al.[12] investigated the effect of electrode diameter on the voltage-arc length characteristic. Over the short range tested, a shift occurs in the curve, Figure 4, without a change of slope. This may be due to an increase in anode drop without any change in the arc column drop. The arc column does appear to have the same physical structure and dimensions in both cases. However, a change in slope is expected to occur if wire sizes are varied greatly because of changing current densities.
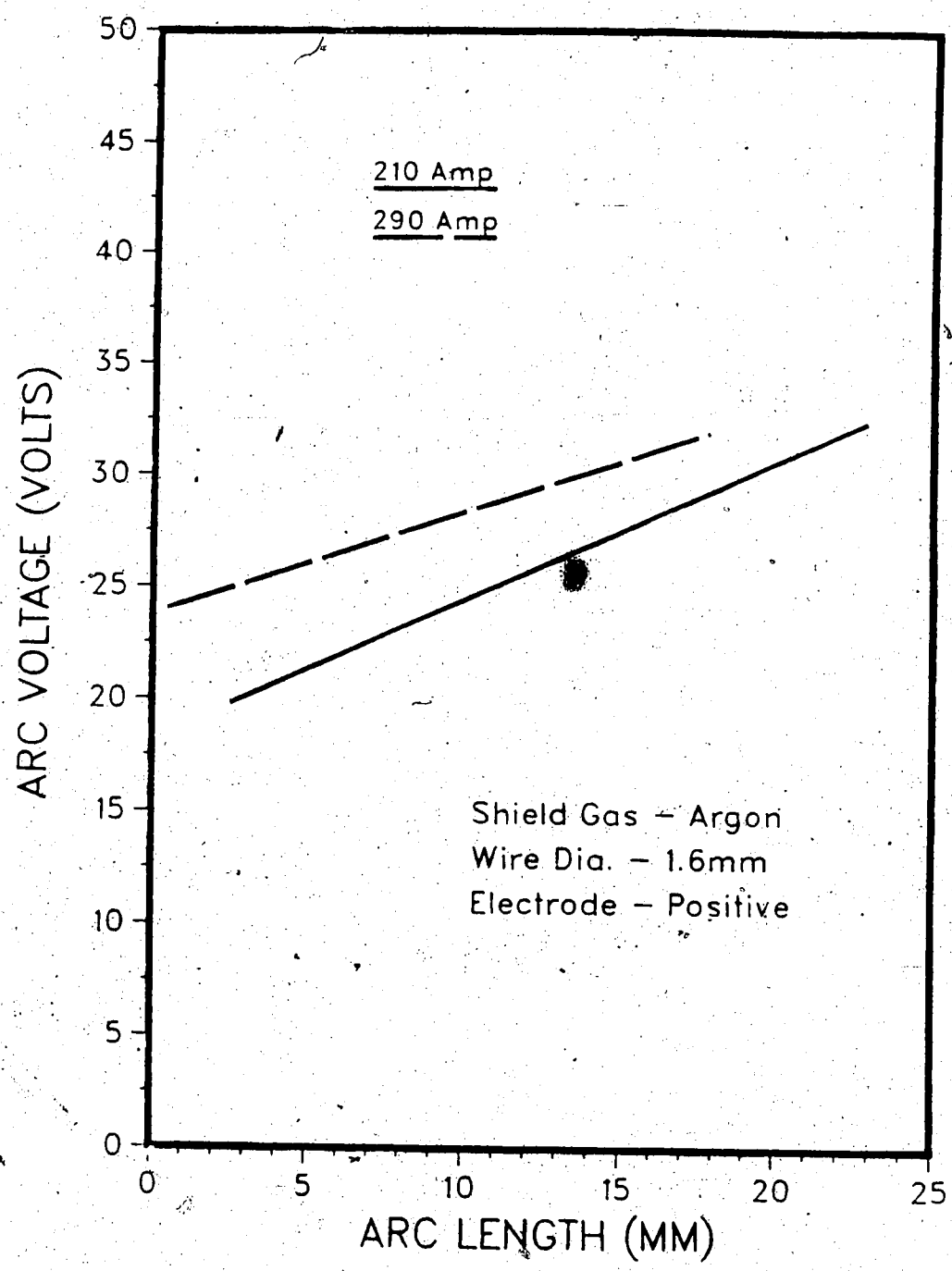
Figure 3. Effect of Current on Voltage—Arc Length
Characteristic (modified from reference 12)
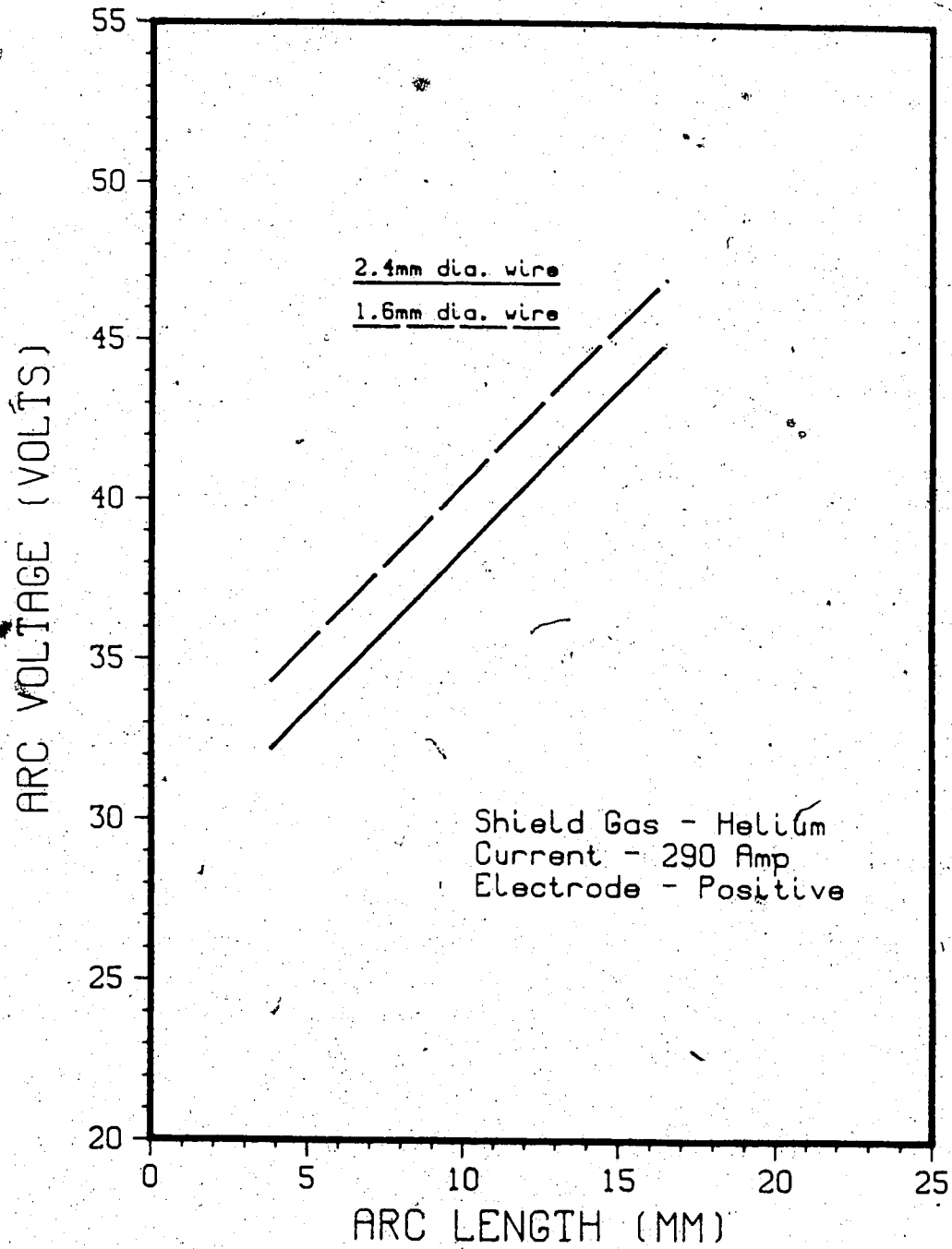
Figure 4. Effect of Diameter of Aluminum Wire
on Voltage-Arc Length Characteristic
(modified from reference 12)

2.2.2 Potential Distribution in the Arc

The potential drop in the arc is not uniform, as illustrated in Figure 1. There is a sharp drop of potential close to the electrodes. In the immediate vicinity of the electrodes the gas can no longer exist at a high temperature because of the cooling effect of the electrodes. The maintenance of the current requires a high potential drop so that the cathode and anode potential drop regions are formed.

The electrons from the column flow into the anode potential drop region which is a very thin layer about 1 micrometre thick adjacent to the anode. However, as they approach the anode the temperature decreases and therefore the density of positive ions, produced by thermal ionization, also decreases, resulting in a negative space charge which is responsible for the anode potential drop. The potential drop in this region is only a few volts but the voltage gradient is very steep. Under the influence of this steep voltage gradient the electrons are accelerated, thereby gaining kinetic energy which is then lost by collisions with the anode. This energy, supplied when the electron stream enters the anode over a very small area, gives the characteristic intense localized heat source that makes the arc so suitable for welding.

Conditions are more complicated at the cathode, for there is the possibility of several processes operating simultaneously, depending on the type of arc. A simplified model, pertaining to a thermionic arc, would be that positive ions travelling towards the cathode are accelerated in the cathode potential drop region, thus acquiring kinetic energy, until they collide with the cathode surface where they become neutralized and give up

their energy of recombination; they may also expend all or part of their kinetic energy, depending on whether they are absorbed by the cathode or reflected from it. Part of the energy thus acquired by the cathode is then used to supply energy equivalent to the work function energy, and the remainder compensates for conduction and radiation losses.

The potential distribution in the arc is generally measured by the use of a probe. Conrady[14] carried out well-controlled probe measurements on aluminum electrode arcs, with currents varying between 50 and 250A, voltage between 32 and 45V, arc lengths between 6 and 24 mm, and 40 mm electrode diameter. The values obtained by Conrady for anode and cathode potential drops are listed in Table 1. The second figure corresponds to larger currents. The results showed the well-established fact that the cathode and anode potential drop varied only slightly with the current.

However, the use of the probe technique for the determination of space potentials in arcs at atmospheric pressure is not entirely justified and can easily lead to biased results because the presence of a probe disturbs the thermal equilibrium in the arc and requires additional electrical energy from the source[15]. For this reason Frett[16] measured the cathode potential drop of aluminum electrode arcs at atmospheric pressure using an adaptation of the method of Bertz and Karrer[17] called the separation method. The cathode potential drop obtained by this method at atmospheric pressure was 11.2 volts as listed in Table 1. The cathode potential drops obtained by the probe method were higher than the values measured by the separation method because it would be physically impossible to insert a probe at a point where the cathode drop would be measured.

Table 1. Cathode and Anode Potential Drops of Aluminum Electordes
Atmospheric Pressure

INVESTIGATOR	CATHODE POTENTIAL DROP (Volts)	ANODE POTENTIAL DROP (Volts)
Conrady	14 - 13	11 -10
Frett	11.2	
Röll	14.5	8 - 11

Röll[18] investigated the dependence of the total voltage (cathode and anode drop) on the current and the arc length using welding arcs with aluminum electrodes of 4 mm diameter. The arc length varied between 6 and 16 mm. The cathode drop showed a remarkable consistency. All values obtained were in the neighborhood of 14.5V regardless of the current, arc length or the composition of the electrode. However, the cathode drop is a function of the ionization potential and the atomic weight of the metal in the cathode and, further, it depends on the special features of the energy level schemes in the atoms, which determine how they react with the electrons, and how they radiate[19]. The anode drop, on the other hand, rises with current and decreases with electrode diameter as mentioned before by Muller et al[12].

2.3. Effect of Welding Speed

An increase in the speed of welding, keeping current and arc voltage constant, generally results in decreased penetration. However, an unexpected effect is that for a given current and arc voltage there is an optimum welding speed, below which penetration decreases due to the large amount of deposited metal raising the level of the weld pool. Tomlinson and Slater[20] showed that changes in welding speed reduce penetration, bead width and reinforcement when current and arc voltage are constant, but have a much greater effect on the width of the weld bead than on the height of the bead or on penetration using bead-on-plate tests with Al-5% Mg electrode wire and plate.

When the welding speed is decreased, the filler metal deposition per unit length increases, and a large, shallow weld pool is produced. The

welding arc impinges on this pool rather than the base metal as the arc advances. This limits penetration but produces a wide weld bead. On the other hand, as the welding speed is increased, the thermal energy transmitted to the base metal from the arc is decreased. Therefore, melting of the base metal is slowed and occurs nearer to the surface of the base metal, thus, decreasing penetration and bead width. As the welding speed is increased further, there is a tendency toward undercutting along the edges of the weld bead. This is because molten metal is pushed back and up into an unstable configuration due to the force of the plasma jet. This deprives the edges of the weld bead of enough molten metal to fill the arc cavity and at high welding speeds the molten metal solidified fast enough to freeze the unfilled configuration, causing undercutting.

2.4   Welding Arcs in Various Shielding Gas Mixtures

2.4.1   Introduction

Since consistent arc behaviour is essential to produce even penetration, regular bead shape and lack of defects such as undercutting and inadequate fusion, arc stability has been one of more actively investigated areas in welding research.   Arc behaviour is strongly influenced by the electron emission characteristics of the metal or metals used as base plates and electrodes, by the type and polarity of current, by the power source design and performance, and by the shielding gas composition. The shielding gas composition has a marked influence on the power density, arc voltage, and thermal efficiency of the welding arc.

Since the 1950's, the inert gas-shielded arc welding processes have almost completely displaced all others for welding aluminum. During this

time, much has been written concerning the nature of the arc in argon, helium and mixtures of argon and helium[21-23]. Little has been published, however, showing the effects of other shielding gas additions such as oxygen, hydrogen, nitrogen, and halogens to argon.

2.4.2 Arcs in Inert Gases

The development of the inert gas-shielded consumable electrode welding process has greatly increased the use of aluminum alloys in welded structures. .Unfortunately, welds made by this process can be porous. Porosity has been attributed to hydrogen in the aluminum-alloy plate and wire, certain types of oxide films on the metal, impurities in the shielding gas, and welding conditions.

Simple cleaning procedures prior to welding can eliminate the plate as a source of contamination. The high standards of purity being maintained by the producers of inert shielding gases have largely eliminated this source of unsoundness in aluminum alloy welds. Likewise, manufacturing techniques are now such that, in general, commercial aluminum products do not contain sufficient hydrogen to make a substantial contribution to porosity. Finally, improvements in the power sources and in the GMAW equipment have done much to eliminate unsoundness arising from arc instability. The greatest source of porosity is hydrogen formed by the reaction of water vapor with molten aluminum.

Over the years, many experiments have been carried out to evaluate the effect of shielding gas composition using argon, helium and mixtures of both. The results showed that the use of a helium-argon mixture shielding gas reduces porosity[24,25]. Several explanations for this have been

proposed. During the welding operation, metal flow is better and oxide removal proceeds more satisfactorily than in either helium or argon alone. In addition, the helium-argon atmosphere produces stable, spray type metal transfer. With the smooth arc, there is less chance for porosity and other flaws to form.

Further studies have revealed that oxygen and chlorine additions to shielding gas reduce porosity and enhance performance whereas nitrogen and hydrogen additions increase weld porosity[2]. However, oxygen additions cannot be used when welding aluminum because refractory oxides form, both at the surface and in the interior of the weld, and therefore inhibit proper metal transfer and deposition, and degrade the mechanical properties by creating flaws, incomplete penetration and porosity.

The next section will discuss the effect on arc stability of additions of chlorine and other halogen gases to argon.

2.4.3 Arcs in Inert Gases with Halogens Added

In non-consumable electrode welding, Matchett and Frankhouser[3] showed that halogen additions to the argon atmosphere used in welding Zircaloy-2 increased penetration. Their studies also showed that the freon additions did not affect the corrosion resistance or the mechanical properties of the weld metal. In plasma welding processes, traces of freon gases containing fluorine and chlorine also increased penetration[4] in Zircaloy-2. As mentioned before, small additions of chlorine to the argon for consumable-electrode welding of aluminum have been used to reduced porosity. However, the effect of chlorine and other halogen gases on arc stability is not well understood.

When the oxidizing gas chlorine is used as an addition to the argon shielding gas in an aluminum GMAW process, chloride ions react with metallic aluminum to give aluminum chloride which, volatilizing at 183 °C, mechanically lifts the aluminum oxide from the surface of the metal. A chlorine level of 0.75% by volume was found to improve arc stability and penetration in electrode negative polarity[5]. However, chlorine is difficult to handle, and causes operator illness because it is highly toxic and causes welding equipment to corrode. Chlorine also leaves a slight film of aluminum chloride on the cool aluminum adjacent to the weld bead. This film, unless removed, could accelerate corrosion. To avoid the use of chlorine gas, several investigators suggested non-toxic gases such as freons to replace chlorine gas[2-5]. Only certain freons containing gaseous combinations of carbon, fluorine, chlorine and bromine can be used. Several other gaseous freons containing hydrogen, e.g. freon 22 ($CHClF_2$) or freon 23 (CHF_3), cannot be used because hydrogen causes porosity in aluminum. Theoretical gas-metal reactions between chlorine, bromine, fluorine and aluminum would produce $AlCl_3$, $AlBr_3$ and AlF_3, respectively. $AlCl_3$ as previously mentioned, volatilizes at 183 °C, AlF_3, volatilizes at 1291 °C, and $AlBr_3$ reaches boiling point at 263 °C. These compounds should not create any problems on the weld pool surface because sufficient heat should be present to promote vaporization in the welding arc.

Bicknell and Patchett[6] investigated the effects of four different freons on an automatic aluminum GMAW process: freon 12 (CCl_2F_2); freon 13 ($CClF_3$); freon 13-B1 ($CBrF_3$); and freon 14 (CF_4). Their study concluded that additions of all four freon gases improved arc stability and weld bead characteristics on both D.C. electrode negative and positive polarity.

However, among the halogen atoms chlorine provided the most marked improvements in arc characteristics, and therefore freon 12 was the best freon gas tested because it contains the highest number of chlorine atoms among the four freon gases tested. They also found that the difference between the effects of fluorine and bromine was minimal. To compare the effect of halogen atoms on arc stability and penetration, Simonik et al.[26] made welds on titanium alloys using different fluxes containing various halides. He also showed that the halogens could be arranged in the following order of increasing penetration effect : fluorine, bromine, and chlorine.

Simonik analysed the phenomena in the arc discharge and hypothesized that halogens entering the zone of the arc discharge may be in four states: as neutral atoms, as molecules, and as positive or negative ions. Along the axis of the arc discharge, where high energy electrons predominate, the most probable state is a neutral atomic state with an extremely small quantity of positively charged ions. Since the probability of the formation of negative ions by the addition of an electron to a molecule of halogen is very much greater than the negative ions formed by the addition of an electron to an atom due to its inability to capture an electron at high temperature, negative ions can appear only at or below the temperature of molecule formation of the halogen, i.e. in the peripheral regions of the arc column. Consequently, reduction of the number of electrons at the periphery lowers the conductivity of the periphery of the arc column, leading to constriction of the discharge.

On the basis of the above hypothesis, it can be suggested that the effectiveness of constriction of the arc column should increase with higher

temperature of halogen molecule formation. At a given high temperature, chlorine shows the highest percentage of molecular state, and bromine and then fluorine come next. The halogens, therefore, should be arranged in the following order of increasing constriction effect : fluorine, bromine and chlorine. This suggestion can be also explained by electron affinity characterized by the proportions of neutral and negatively charged particles at a temperature below the temperature of molecule formation. The higher the electron affinity the greater the proportion of negatively charged particles. Chlorine, 3.76 eV, has higher electron affinity than bromine, 3.54 eV, and fluorine, 3.58 eV. Again, the difference between the effects of fluorine and bromine on arc characteristics is minimal because their electron affinities are very similar. On the whole, it can be concluded that the increase of penetration is a consequence of increased constriction of the arc column without changes of current.

2.5 The Transfer of Material Across the Arc

2.5.1 Introduction

The advent of the gas-shielded consumable electrode processes and general availability of high-speed cameras has greatly increased progress in the understanding of metal transfer. The phenomena of metal transfer in arc welding and especially the governing mechanisms received considerable attention during the late 1950's and early 1960's. Needham[27] studied the burnoff rate and drop transfer rate for aluminum GMA welding, and showed that there is a transition current (which varies with wire diameter) below which the transfer is in the form of large droplets that appear to detach by gravity, and above which the drops are projected across the arc

(spray or projected transfer). At the transition current there is a discontinuity in both the burnoff rate/current and droplet rate/current curves. It was found that the drops have a velocity and an acceleration when they detach, and are further accelerated in their passage across the arc. The axial displacement of the drop increases exponentially with time, and there is a time constant which varies with current. In GMA welding of steel with a steel electrode, there is another transition at a higher current, about 250A, when the pencil-point tip suddenly transforms into a relatively long cylinder of liquid metal from the end of which a stream of fine drops is projected (streaming transfer)[28]. At a still higher current the cylinder transforms into a rotating spiral (rotating transfer).

The geometric form of the drop at the electrode tip depends on, amongst other factors, the polarity. The work on aluminum and steel electrodes discussed above was all done with electrode positive. When the electrode is negative metal transfer characteristics are completely different. Cooksey[29] investigated metal transfer of aluminum in argon with electrode negative. His study showed that the drops are repelled from the plate because of a localized unbalanced electron pressure at the cathode spot where electrons are produced.

2.5.2 Transfer Mechanism in the Welding Arc

In the initial stages of globular transfer the plasma jet forces are not strong enough to overcome the surface tension of the material detaching the molten tip because the current density and current density gradient are low. The molten end, therefore, grows in size. The current density at the electrode is further reduced by the increasing size of the globule and the

forces weaken. Finally, the globule's weight itself plays a large part in overcoming the surface tension in the neck and the globule breaks from the rod and drops to the plate. When the globule breaks from the wire, the arc immediately transfers to the wire end. Momentarily the current density gradient is quite high, resulting in a plasma jet impinging on the back of the globule.

The plasma jet force at this current is not strong enough to influence the globular drop in its flight to any great extent because of the large material mass. As the current is increased a critical point is reached where the arc surrounds the tip of the electrode and the plasma jet force (skin friction) is just large enough to detach the droplet at its initial small size. If the force is just too low to effect detachment the droplet will grow in size to globular dimensions because, as before, the force decreases with increase in size of the globule. Thus a marked transition from globular to spray transfer will occur over a very small range of current.

At even higher currents still the weld pool contour takes on the shape known as fingering (i.e., much deeper penetration at the center than at the edges). This is caused by the formation of an ionization core in the arc column and the temperature profile of the arc column is imaged by the molten region of the plate. The high temperature core in the column with its associated high electrical conductivity causes a marked increase in the magnetic pinch forces and thus an increase in the plasma jet force. This force can become so high that material is actually blown out of the weld pool, but just before this stage is reached, if the argon gas flow is not properly well covering the discharge, the jet will suck air into itself and

this into the weld pool, thus causing oxidization in the pool and the formation of flaws.

At very high currents the welding arc becomes erratic because the feed wire starts vibrating and the arc goes, into a form of rotation. This occurs because the high current flowing in the feed wire causes the wire to become plastic due to the I^2R drop along the wire. The reaction force from the plasma jet at the end of the wire creates enough forces on the welding wire end to oscillate and, as the wire melts back, the droplets entering the jet will be ejected at various angles according to the direction of the jet at the time to create puckering or rotating spray transfer.

2.5.3 The Drop Transfer Rate and Size

Since the drop transfer rate provides a useful means of characterising the nature of metal transfer for any particular process and is relatively easy to measure, experimental results are readily available. With the GMAW process, as the wire feed rate is reduced, the current drops accordingly. The transfer frequency also falls, but somewhat more rapidly than the current, so that there is an increase in the mean droplet size. Aluminum differs from steel in that there is a transition current below which transfer is in relatively large drops at a slow rate, and above which drops are small and have an initial velocity and acceleration. For example, in the case of a 1.6 mm diameter aluminum wire, the large drops range from 6 mm in diameter to 3.5 mm, and above the transition they are 2 mm diameter and smaller[30]. The transition current is just over 100A for 1.6 mm diameter aluminum wire. However, if the diameter of the electrode is changed the transition current will also be changed.

An understanding of the transition from globular to spray transfer, and of the decrease in particle size with current, requires a more detailed analysis. When metal transfer takes place vertically downwards, the force due to the combination of gravity and the plasma jet acts to detach the drop from the electrode. If the force is sufficient to overcome the restraining force of surface tension of the electrode material, the drop would then be detached as given by:

$$1/2 \; F \; (\; 1+ \; (\; R_d^2 - R_e^2 \;) \; / \; R_d^2 \;) \; + \; mg \; = \; 2\pi R_e \gamma \qquad (2)$$

where F is the plasma drag force exerted on the drop (N)

R_d is the radius of the drop (m)

R_e is the radius of the electrode wire (m)

m is the mass of the droplet (kg)

g is the acceleration due to gravity (m/sec^2)

and γ is the surface tension of the electrode material (N/m).

The first term of the left hand side equation is the force exerted by the plasma jet while the second term is the force due to gravity. Since the force F which is exerted on the drop increases with the velocity of the plasma jet which also increases with current, the force due to the plasma jet decreases with a decrease in current while the restraining force remains constant. Therefore, below the transition current the relative contribution of the force of gravity is very large compared with that of the plasma jet. Consequently, the drop size is increased. However, above the transition current the reverse is true. The experimental results of Needham and Smith[30] (Figure 5) show the variation in drop size with current with both electrode positive and electrode negative. Both curves show not only the
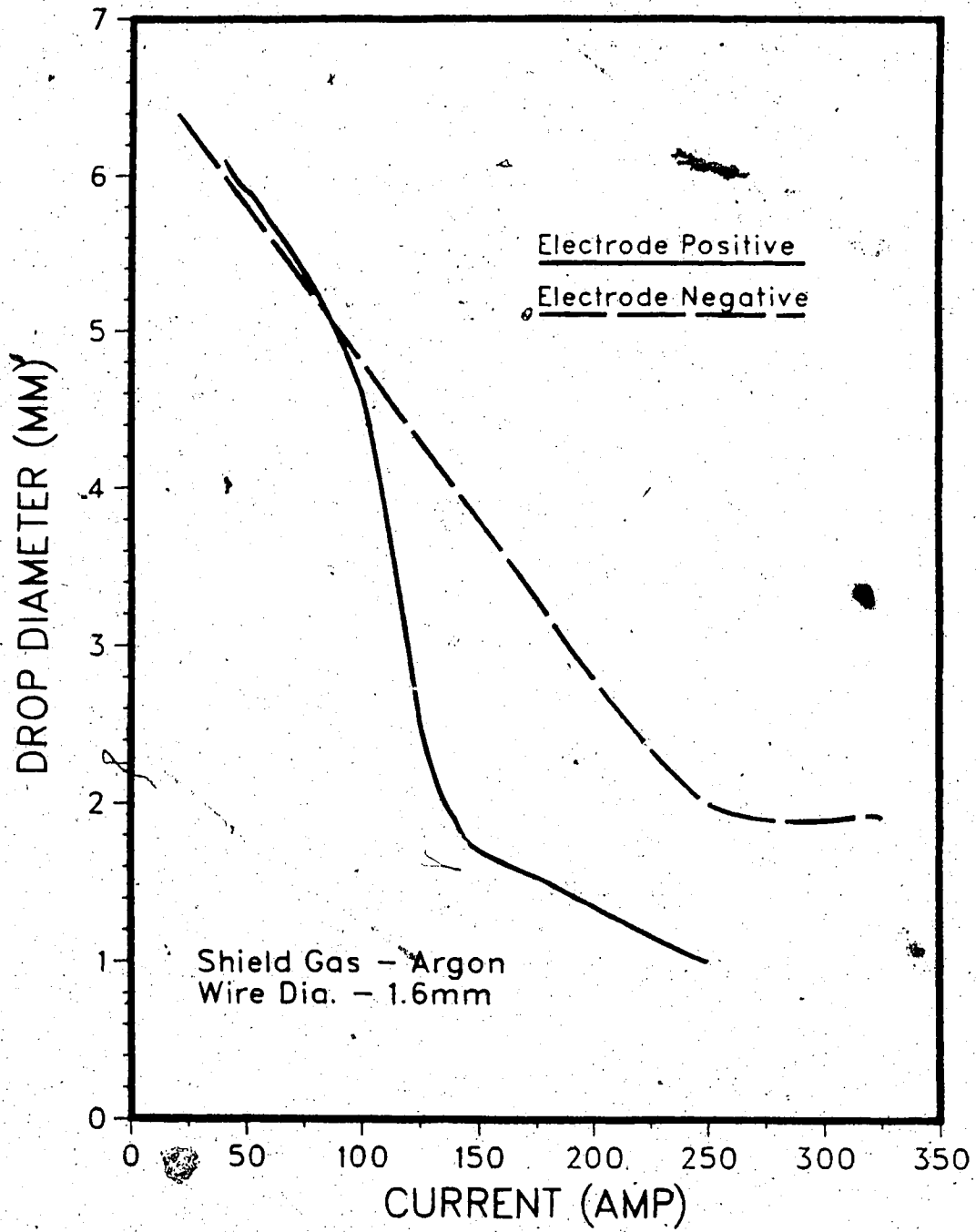
Figure 5. The Variation in Drop Size with Current
with Both Electrode Polarities
(modified from reference 30)

marked transition in drop size at the transition, current but also decreasing drop diameter with increasing current. The transition in droplet size with electrode negative is not so marked as with electrode positive.

The drop transfer rate is the burnoff rate (kg/amp-sec) divided by the drop volume which can be expressed as:

$$D = 0.0294 \ b_a \ I \ ((\ 1 + (\ \mu_o \ I^2 \ / \ 2 \ \pi^2 \ R \ \gamma))^{3/2} \ / \ \rho_m \ R^3 \quad (3)$$

where b_a is the burnoff rate (kg/amp-sec)

   I is the current (amp)

   μ_o is the permability of free space (henry/m)

   ρ_m is the density of the electrode material (kg/m^3)

and R is 1/2 (R_d + R_e) (m).

Figure 6 shows the results obtained by using Equation 3 and the measured values[30]. The calculated curve is steeper over the same current range than the measured results but they are reasonably close together. The difference between these two curves is attributed to the uncertainty of the assigned values to the density, burnoff rate, and surface tension in Equation 3. Because these parameters are markedly dependent on the temperature, assigning actual values is very difficult.

2.5.4 Transfer of Drops Across the Arc

A number of workers have shown that in GMA welding the drops, having detached from the electrode, are further accelerated across the arc by the high-velocity plasma jet. The force F exerted on the drop placed in this high-velocity plasma jet is obtained from the drag coefficient C_d

$$C_d = 2 \ F \ / \ \pi \ v^2 \ \rho_g \ R_d^2 \quad (4)$$
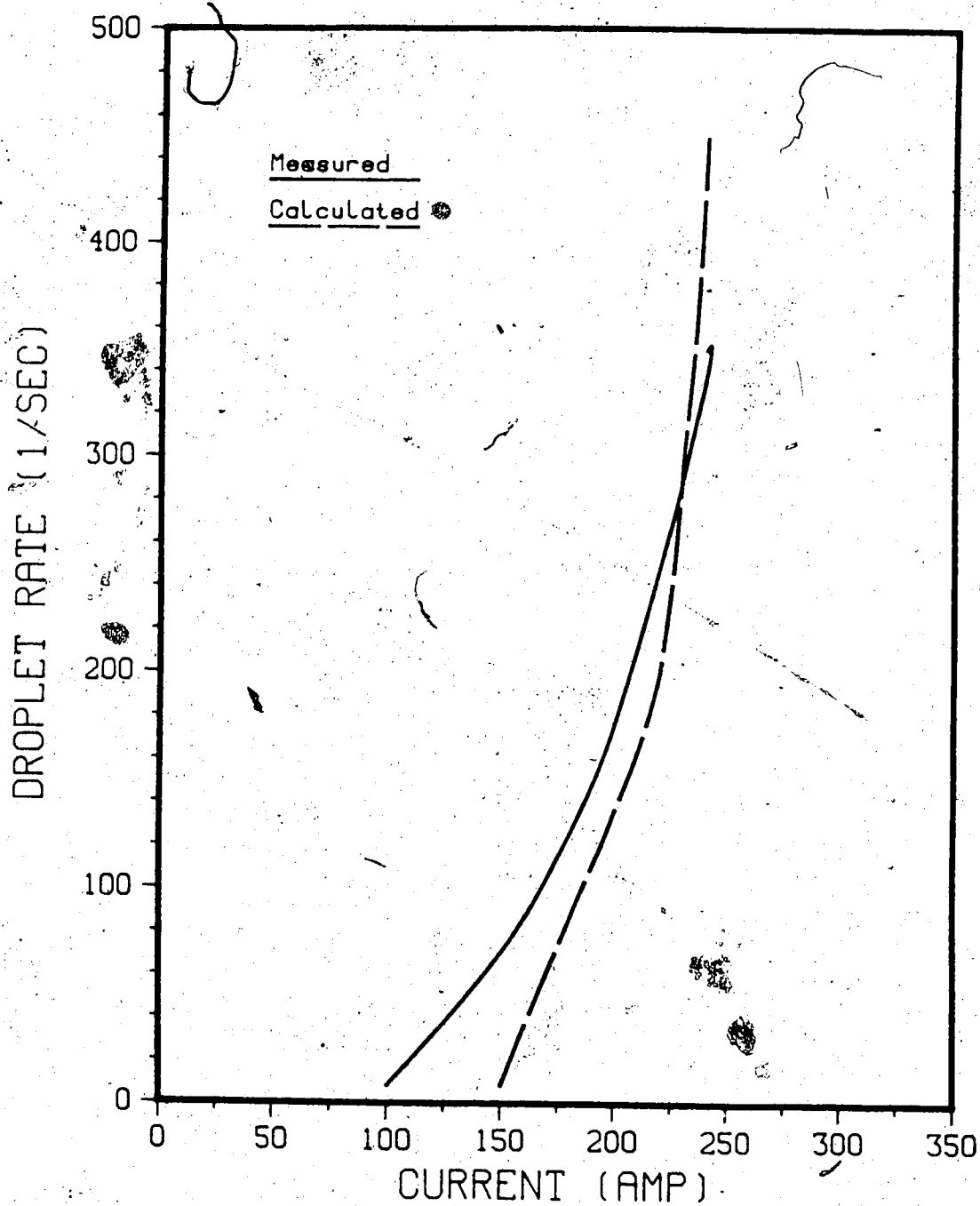
Figure 6. Droplet Rate for 1.6mm Diameter Wire,
in Argon, Electrode Positive
(modified from reference 30)

where v is the axial velocity of the plasma jet, and ρ_g is the density of the flowing medium. C_d is in turn a function of the Reynolds number R_e of the flow. Over the range of Reynolds numbers that occur in the present work (i.e., 10 to 100)[27], this relation can be expressed approximately as:

$$C_d = 64 \ / \ R_e \tag{5}$$

where $R_e = R_d \ v \ / \ \upsilon$, and υ is the kinematic viscosity of the flowing medium. The axial velocity of the plasma jet used in both the drag coefficient and Reynolds number can be calculated by using the Squire Model:

$$v = 3 \ \mu_0 \ I^2 \ / \ 64 \ \pi^2 \ \eta \ r_0 \tag{6}$$

where η is the dynamic viscosity of the flowing medium, and r_0 is the distance from the electrode tip.

The acceleration of drops due to the plasma stream in the arc column and the force on the drop may therefore be obtained by first calculating the Reynolds number and the corresponding drag coefficient:

$$F = \pi/2 \ v^2 \ \rho_g \ R_d^2 \ C_d \tag{7}$$

$$a = 3/8 \ (v^2 \ \rho_g \ C_d \ / \ R_d \ \rho_m) \tag{8}$$

For example, the acceleration of drops across the arc for GMA welding of steels, 1.2 mm diameter electrode and 12 mm arc length at 200A is calculated to be 46.6 m/sec^2.

2.6 Survey Summary and Conclusions

Shortly after the gas tungsten-arc process provided a great success in welding aluminum alloys, attention was given to developing a modification of the process that would provide filler metal for more efficient filling of a groove or joint. One of the early changes was to simply replace the tungsten electrode with a consumable metal wire to serve as the electrode and provide the filler material. Since then, the GMAW process has been widely used for welding aluminum and its alloys. The high demand for its use in aluminum fabrication stimulated rapid strides toward improving the quality of the weld metal deposited by the process. Within a short period of time, factors responsible for the porosity in the weld metal were established and the means for their elimination quickly adopted. These included improvement in equipment design, cleanliness of the surface of the core wire, purity of the shielding gases, adequacy of gas flow and proper welding techniques. With these improvements, the process readily demonstrated its ability to deposit good quality weld metal. However, uncertainty still remains in regard to the effects of shielding gas composition on arc stability. While numerous researchers have studied the nature of the arc in argon, helium and mixtures of both, investigations related to the effect of active additions to the shielding gas on arc behaviour are limited.

Although it has been shown that chlorine improves arc stability, chlorine is difficult to handle, and causes operator illness because it is highly toxic and causes weld equipment to corrode. To avoid the problem of adding chlorine directly to the argon shielding gas, non-toxic freon

gases containing fluorine, bromine and chlorine have been proposed to replace chlorine gas. It has been reported that additions of freon gases to the argon shielding gas increase arc stability and penetration on both D.C. electrode polarities. It has further been reported that among the halogen atoms chlorine provides the most marked improvements in arc characteristics. Consequently it was decided to investigate freon containing higher numbers of chlorine atoms.

To date, no work has been published on the use of freon 11 (CCl_3F) with argon as a shielding gas for welding aluminum alloys on both D.C. electrode negative and positive polarity with the GMAW process. The major goal of the following experimental studies was to compare the effects of the various freon additions with that of pure argon shielding gas on arc stability and characteristics using both D.C. electrode polarities. Another goal in this project was to determine optimum welding conditions for both D.C. electrode polarities using an argon-2% freon 11 shielding gas mixture and evaluate the mechanical properties of the resulting weld metal deposits.

3.   Experimental Procedure

3.1   Materials

The plates used for this work were 5086 aluminum alloy with strain hardening only (H116). All material came from bars initially 183 by 7.6 by 1.3 cm (72X3X1/2 in), which was cut into individual plates (30X7.6X1.3 cm). These plates were then degreased with ethanol and mechanically stainless wire brushed before each test. The chemical composition and mechanical properties of this alloy are presented in Tables 2 and 3, respectively[30].

3.2   Optimum Shielding Gas Mixture and Welding Conditions

3.2.1   Experimental Setup

All bead runs were laid automatically using a fixed automatic GMAW torch. Test beads about 200 mm long were deposited from a single reel of 1.6 mm dia. 5356 aluminum alloy using both electrode positive and electrode negative operation. The distance between contact tube and wire tip was always 25 mm, and the total shielding gas flow rate was 15 L/mm at 137.8 kPa.

To determine an optimum shielding gas composition and welding conditions, the following welding parameters were varied: arc voltage, current, wire feed rate, and welding speed. Voltage and current readings were taken from conventional meters during specimen welding. Since current is a direct function of wire feed rate, it was controlled by adjusting the wire feed rate.

Table 2.   Chemical Composition of 5086-H116 Aluminum Alloy
(wt%) (modified from reference 31)

Mg	3.5 - 4.5		Cu	0.1
Mn	0.2 - 0.7		Zn	0.25
Cr	0.05 - 0.25		Ti	0.15
Si	0.4		Others	0.15
Fe	0.5		Al	Rem.

Table 3.   Mechanical Properties of 5086-H116 Aluminum Alloy
(modified from reference 31)

Ultimate Tensile Strength (MPa)	275.6
Yield Strength (MPa)	192.9
Elongation (%)	10

To compare the effects of the various freon additions, the total shielding gas flow rate had to be monitored carefully. When pure argon and argon-freon 12 shielding gas mixtures were used, controlling the appropriate gas flow rate of each component was easily carried out by using a four tube flowmeter and mixer. However, to mix freon 11 with argon a recycle hot fluid bath had to be used to heat freon 11 because the boiling point of freon 11 is 23.82 °C. The heating ensures that the outlet pressure is more than 137.8 kPa to avoid a reverse flow.

3.2.2 Initial Experimentation

As a means of comparison, initial tests were carried out with three different shielding gas mixtures; pure argon, argon-2% freon 12 and argon-2% freon 11. Freon addition at 2% by volume was chosen because previous work[6] had showed that freon 12 at 2% by volume was the optimum shielding gas mixture, establishing a balance between arc stability and surface appearance. Since the total shielding gas flow rate was 15 L/min, 2% freon addition was 300 cc/min. The other procedural conditions were: arc voltage, 25V; welding current, 200A and d.c. electrode positive; welding speed, 425 mm/min. Cross sections of weld beads were polished and etched (10% NaOH) for comparison.

3.2.3 Optimum Welding Conditions for Both Electrode Polarities

Having compared the shielding gas mixtures, three variables, arc voltage, current, and welding speed, were varied as shown in Table 4 to determine optimum welding conditions for both electrode positive and electrode negative using an argon-2% freon 11 shielding gas mixture.

Table 4. Tests for Finding Optimum Welding Conditions for Both Electrode Polarities

BEAD ON PLATE NO.	ELECTRODE POLARITY	VOLTAGE (Volts)	CURRENT (Amp)	SPEED (mm/min)
3	+	26	200	1000
7	+	26	300	1000
9	+	26	325	1000
10	+	26	325	600
12	+	26	325	400
14	-	26	200	400
15	-	28	200	400
16	-	28	200	600
17	-	28	200	800
18	-	28	200	1000

Cross sections of weld beads were polished and etched (10% NaOH) for comparison.

3.3 Mechanical Properties of Weld Metals

3.3.1 Groove Welding

To assess the mechanical properties of weld metals two types of single-V grooves, as illustrated in Figure 7, were tested and compared using the following welding conditions: electrode polarity, positive; shielding gas, argon-2% freon 11; arc voltage, 26V;   current, 200A; welding speed varying, from 230 mm/min to 400 mm/min.

Using the type 2 groove, the effects of welding current and speed on penetration and bead shape were studied and metallography (X-section) was used to compare weld profiles. After finding the optimum welding conditions, a 1% freon 11 addition to the argon and pure argon shielding gas mixtures were tested and compared with argon - 2% freon 11.

3.3.2 Tensile Testing

All tensile specimens described in Figure 8 (other than that from the base plate) were taken from butt welded plates (see Figure 9). The specimen dimensions are described in Figure 8. The welding conditions used to make the butt welded plates were: edge preparation, type 2; arc voltage, 26V; electrode polarity, positive; welding speed, 240 mm/min; current, 300A except for pure argon shielding gas, 250A.

35°

6.5 mm

6.5 mm

Type 1

35°

8.0 mm

5.0 mm
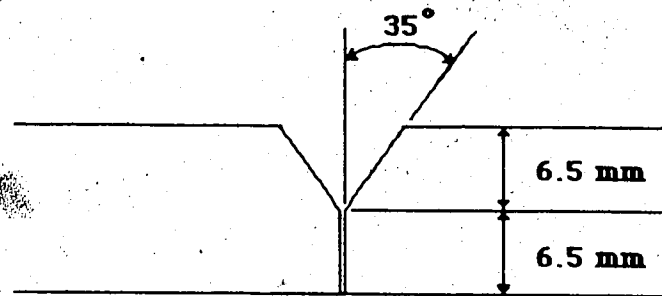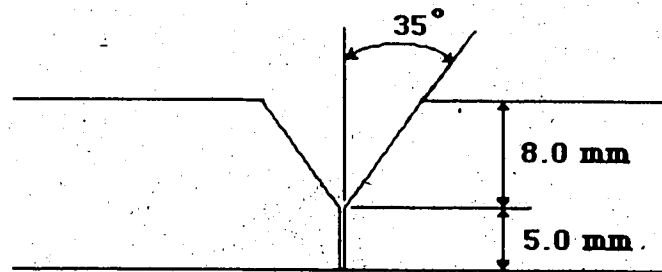
Type 2

Figure 7. Two types of Single-V Groove Preparation
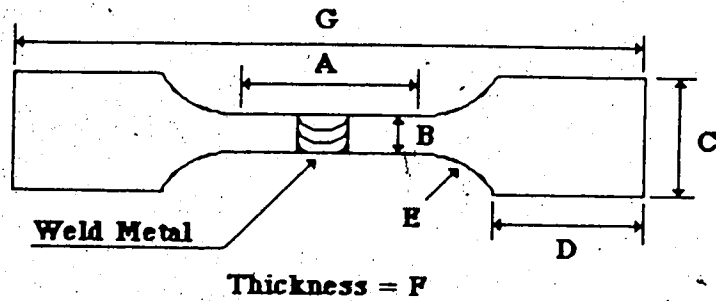
A (Gauge Length) = 50.8 mm

E = 18.0 mm dia.

SPECIMEN	B	C	D	F	G
5086 Baseplate	7.8	25.0	40.0	12.9	143.7
Pure Argon Transverse with Reinforcement Removed	19.7	25.0	40.0	6.2	143.7
Argon + 2% Freon 11 All Weld Metal Machined	12.6	25.0	40.0	11.9	152.5
Argon + 2% Freon 11 Transverse with Reinforcement Removed	12.1	25.0	40.0	11.8	152.5
Argon + 2% Freon 11 Transverse with Reinforcement	16.5	25.0	40.0	12.8* 16.9**	152.5
Argon + 2% Freon 11 Transverse with Reinforcement Large Specimen	50.8	101.6	127.0	12.7*	445.0

*: Base Metal
**: Weld Metal
All dimensions are in mm.

Figure 8. Dimensions for Tensile Specimen

↓ 1 mm
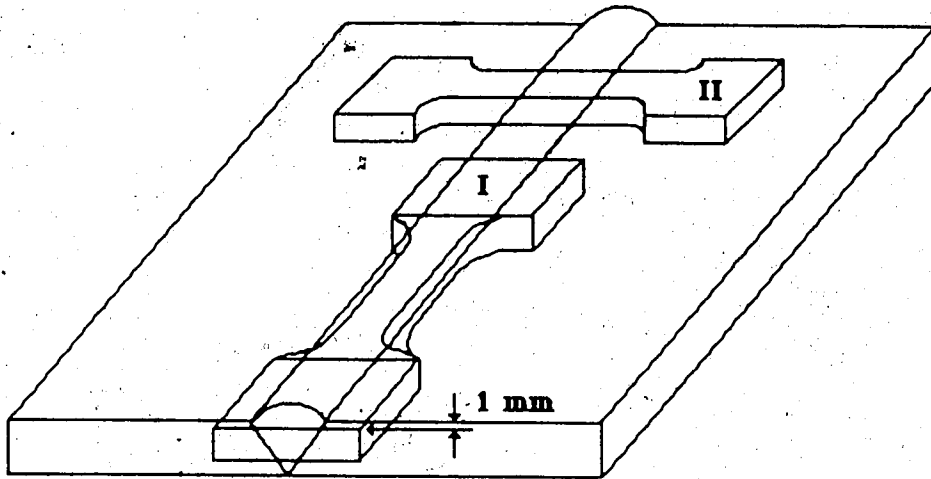
Type I: All Weld Metal Tensile Specimen
Type II: Transverse Tensile Specimen

Figure 9. Location of Tensile Specimen

3.4 Metal Transfer Characteristics

The droplet transfer process for both polarities was analyzed using a high speed video camera at 2000 frames per second. The electrode tip, crater, and transferring metal were silhouetted by a xenon backing light (1 kW), with the camera set at right angles to the transverse and using a long focus lens (200 mm focal length) to give a near full size picture of the arc on the film. The welding conditions for the bead runs are described in Table 5. The measured variables were visible arc length, displacement of the drop against time, and frequency.

3.4.1 Visible Arc Length

To determine the influence of different shielding gases on arc length for a given arc voltage, an arc was established using three different shielding gas mixtures as-shown in Table 5. The true arc length could not be measured directly because there appeared to be a fraction of the arc below the plate in a crater travelling with the visible portion of the arc. The visible arc length (the distance between the top of the electrode and the surface of the base metal) immediately following the detachment of the drop, was measured on a T.V. monitor for each run. The actual diameter of the electrode wire was compared to the diameter on the screen to obtain real arc length values.

These visible arc length measurements were then plotted against voltage for both polarities as shown in Figures 27 and 28 (pages 60 and 61). Although images of the arc varied within 0.5 mm in length due to

Table 5 Welding Conditions Used for Determining Metal Transfer Characteristics

ELECTRODE POLARITY	WELDING SPEED (mm/min)	SHIELDING GAS	CURRENT (Amp)	VOLTAGE (Volts)
Positive	240	Pure Argon	250	26
				27
				28
				29
			300	29
				31
				33
		Argon + 2% Freon 12	300	26
				27
				28
				30
				32
		Argon + 2% Freon 11	300	26
				27
				28
				29
				30
Negative	800	Argon + 2% Freon 12	200	26
				27
				28
				29
		Argon + 2% Freon 11	200	26
				27
				28
				29

continual wire movement and indefiniteness of the arc extremities, this effect on the overall relationship is minor. However, two corrections must be applied to the recorded voltage. The voltage drop was measured by using a voltmeter from the work piece to the point where both terminals were connected to the voltmeter. The second correction was made for the voltage drop in the electrode stickout. The voltage drop in the electrode stickout was calculated using the following values: current, 300 amperes; electrical resistivity at 315 ^{0}C, 2.68 X 10^{-7} ohm·m; electrode stickout, 25 mm; electrode diameter, 1.6 mm. These two corrections were then subtracted from the recorded voltage to obtain the actual voltage.

3.4.2   Velocity and Acceleration

Since it was essential to accurately establish the displacement-time function, the measurement of drop displacement was achieved by measuring the frame-by-frame displacement of the droplet in free flight and by using the bottom of the gas shielding cup as the reference point. Each measurement was taken from this reference point to the top of the droplet. Actual displacement values were obtained by using the same method as before. The drop velocity and acceleration were then derived from the basic distance vs time relationship.

3.4.3   Frequency and Bead Width

The frequency of the droplet transfer was determined from the time interval between two consecutive drop detachments from the electrode wire. Knowing the frequency and wire feed rate, the diameter of actual size of the equivalent sphere was calculated.

The average measurements of the salient dimensions of the beads made in this work are represented graphically in Figures 21 and 22 (pages 54 and 55). All measurements were made on a cross section of weld beads with a Vernier caliper:

4. Results and Discussion

4.1 Initial Experimentation

As a means of comparison, initial tests were carried out using identical welding conditions for three different shielding gas mixtures: pure argon, argon - 2% freon 12 and argon - 2% freon 11. The resulting weld profiles are shown in Figures 10A through 10C. Under the standard welding conditions used pure argon (Figure 10A) produced a rounded bead with the least penetration. Metal transfer was fairly smooth with almost no spatter. However, since 5356 filler wire containing high vapour pressure elements such as magnesium was used, the smooth metal transfer was interrupted occasionally at irregular intervals because of the explosive disruption of the molten droplet in mid-flight.

Using the same welding conditions, argon - 2% freon 12 and argon - 2% freon 11 shielding gas mixtures produced much better penetration than that of pure argon. However, the amount of spatter was increased considerably as was the amount of fume produced. Although the argon - 2% freon 12 gas mixture caused wider and slightly deeper penetration than argon - 2% freon 11 gas mixture, the weld profile was irregular due to arc length fluctuations. The resulting bead surface was also covered with a tenacious black deposit, probably MgF_2 because MgF_2 has a high melting point of 1261 ^0C and a boiling point of 2239 ^0C. Argon - 2% freon 11 caused the arc to become very stable, resulting in a remarkable surface and a highly regular weld profile. There was no evidence of the black deposit on the surface.
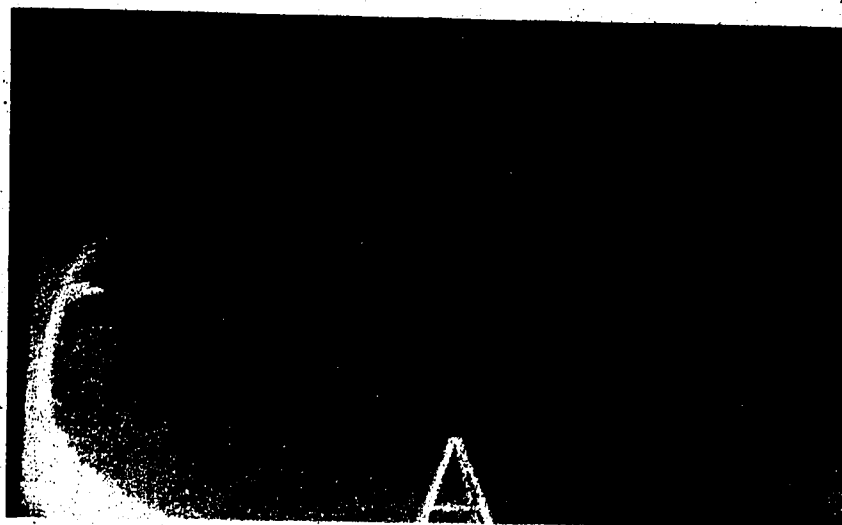
Figure 10A. Electrode Positive: Pure Argon (3.7X)

Figure 10B. Electrode Positive: Argon - 2% Freon 12 (3.7X)

Figure 10C. Electrode Positive: Argon - 2% Freon 11   (3.7X)

Having compared the shielding gas mixtures using electrode positive polarity, pure argon and argon - 2% freon 11 gas mixtures using electrode negative polarity at 28 volts, 200 amperes and 600 mm/min were compared as shown in Figures 11 and 12, respectively. Pure argon produced a very unstable welding condition. Arc length fluctuated erratically to produce random misplaced droplets and therefore surface regularity was very poor. The resulting bead was mostly non-uniform with no penetration into the baseplate. By adding 2% of freon 11, the arc was stabilized considerably and penetration was increased compared to that of pure argon. However, penetration was still minimal and bead profile was poor with excessive crown height. The lack of penetration is caused by insufficient heat being generated in the baseplate. Since aluminum is a poor thermionic emitter, most of the heat is generated in the electrode when electrode negative polarity is used, and therefore the high electrode melting rate in conjunction with a low fusion width produces excessive crown height.

4.2. Optimum Welding Conditions for Both Electrode Polarities

Having established that argon - 2% freon 11 gas mixture produced the best results among the three different shielding gas mixtures, its optimum welding conditions for both electrode polarities were assessed. Weld penetration and bead geometry are affected by several variables:

1) Welding amperage

2) arc voltage

3) travel speed

4) electrode extension
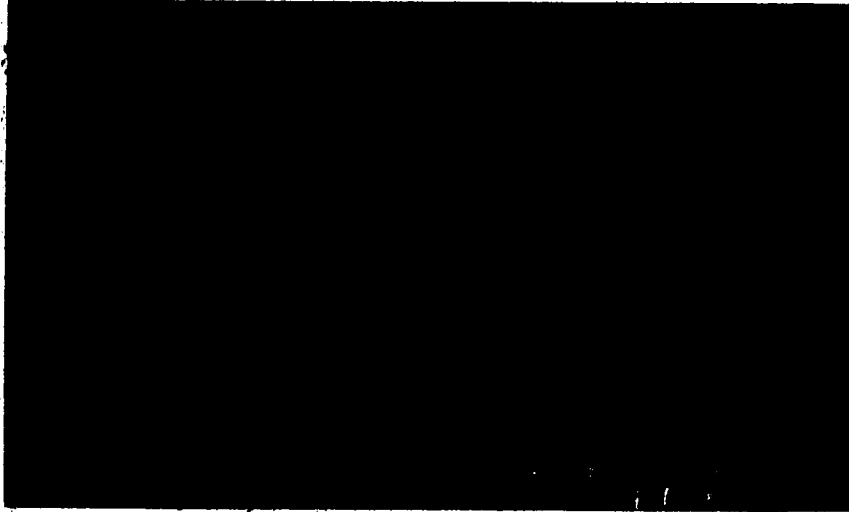
5) electrode inclination

Figure 11. Electrode Negative: Pure Argon, 28 volts, 200 amperes and
600 mm/min (4.4X)

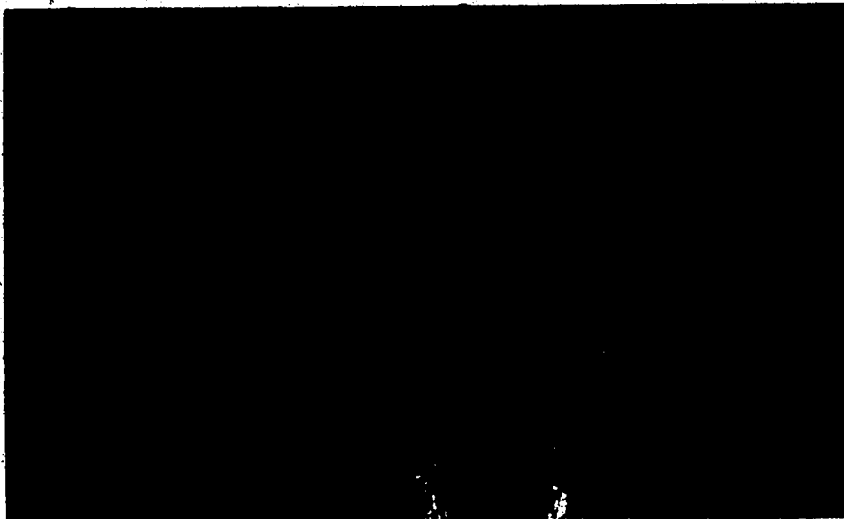Figure 12. Electrode Negative: Argon - 2% Freon 11, 28 volts, 200
amperes and 600 mm/min (3.7X)

6) electrode size

7) weld joint position.

Of course, shielding gas selection also influences weld penetration and bead geometry, as discussed previously. In this experiment, the effects of the first three variables, welding amperage, arc voltage and travel speed, were studied using both electrode positive and negative polarity. Other variables were held constant throughout the experiment.

When all other variables are held constant, the welding current was found to increase non-linearly with an increase in the electrode feed rate. Also, an increase in welding current resulted in:

1) an increase in the depth and width of the weld penetration

2) an increase in the deposition rate

and 3) an increase in the size of the weld bead.

These effects are well illustrated in Figures 13 through 15 for electrode positive polarity.

Figures 15 through 17 reveal that increasing the speed of welding while keeping the current and arc voltage constant results in decreased penetration and bead width. However, for a given current and arc voltage there is an optimum welding speed below which penetration decreases but bead width still increases. This is because the filler metal deposition per unit length increases, and therefore the welding arc impinges on a weld pool rather than on the base metal as the arc advances. The optimum welding speed for electrode positive polarity was found to be 400 mm/min at 26 volts and 325 amperes. The welding speed of 400 mm/min produced

Figure 13. Electrode Positive: Argon - 2% Freon 11, 26 volts, 200
amperes and 1000 mm/min   (3.7X)

Figure 14.   Electrode Positive: Argon - 2% Freon 11, 26 volts, 300
amperes and 1000 mm/min   (4.7X)

Figure 15. Electrode Positive: Argon - 2% Freon 11, 26 volts, 325
amperes and 1000 mm/min (4.4X)
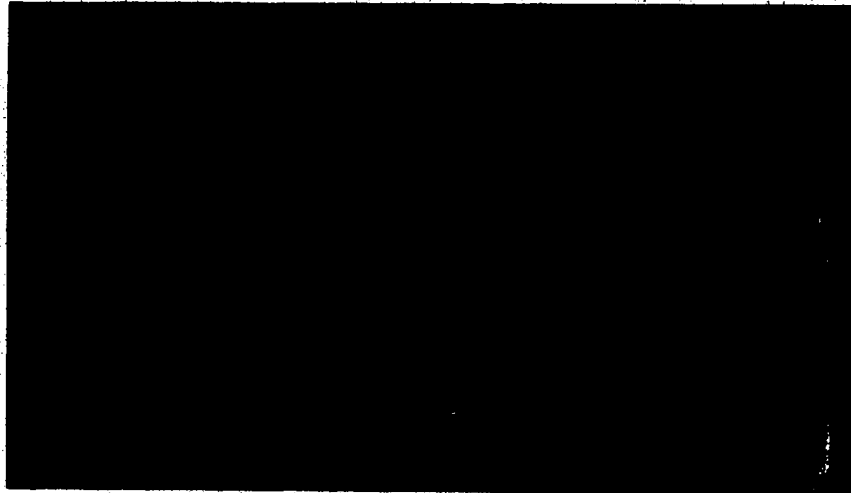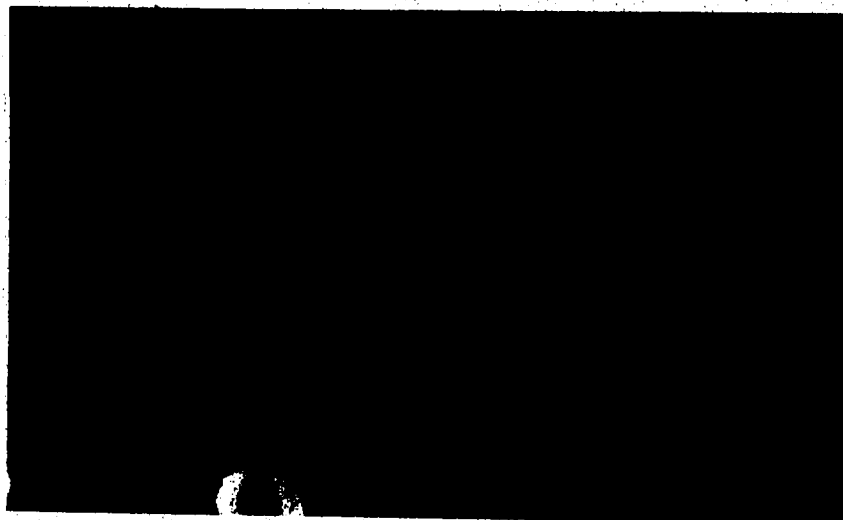
Figure 16. Electrode Positive: Argon - 2% Freon 11, 26 volts, 325
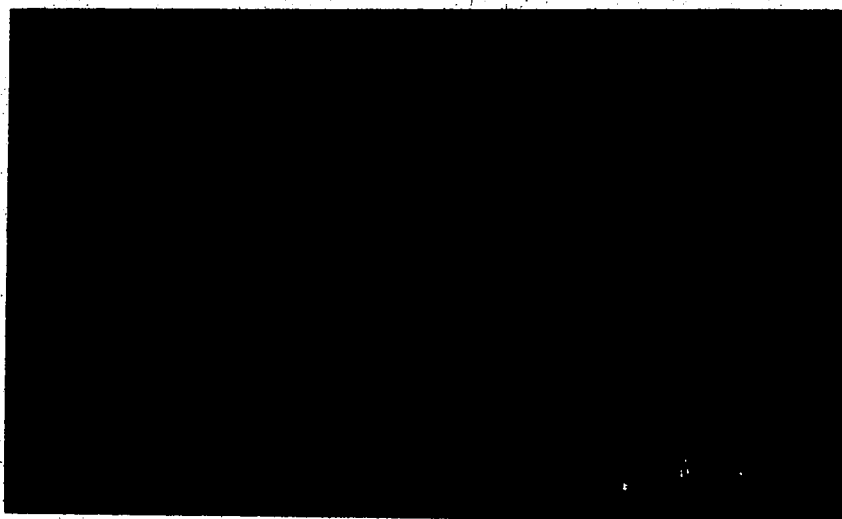amperes and 600 mm/min (3.4X)

Figure 17. Electrode Positive: Argon - 2% Freon 11, 26 volts, 325 amperes and 400 mm/min (3.5X)

a good weld profile regularity although the penetration was not deeper than at 600 mm/min. At a welding speed of 1000 mm/min, undercutting starts to appear along the edges of the weld bead as shown in Figure 15. Figures 12 and 18 to 20 also show the same effects of welding speed for electrode negative polarity.

The effect of arc voltage on weld profile is dependent upon a variety of factors, including the metal thickness, the type of joint, the position of welding, the electrode size, the shielding gas composition, and the type of weld. A voltage increase generally tends to flatten the weld bead and increases the fusion width due to an increase in arc length. Reduction in voltage results in a narrower weld bead with a high crown and deeper penetration. However, when a poor thermionic emitter such as aluminum is used, the results are not the same. In aluminum, a voltage increase tends to increase the fusion width in electrode positive polarity (Figure 21), while in electrode negative polarity, the fusion width becomes relatively constant regardless of arc voltage (Figure 22). Unlike the GTAW process, more heat is generated at the cathode surface by producing the electrons from a poor thermionic emitter. As a result, in electrode positive polarity, a high heat input on the baseplate tends to make a large weld pool on the surface and it becomes easier for the baseplate to produce the electrons. Therefore, an increasing in arc voltage increases the arc length and fusion width.

In electrode negative polarity, however, there is just enough heat input to break the same amount of oxides on the surface regardless of arc voltage, and the anode area becomes relatively constant. The fusion width, therefore, also becomes constant. The resulting weld profiles (electrode

Figure 18. Electrode Negative: Argon - 2% Freon 11, 28 volts, 200 amperes and 400 mm/min (3.5X)
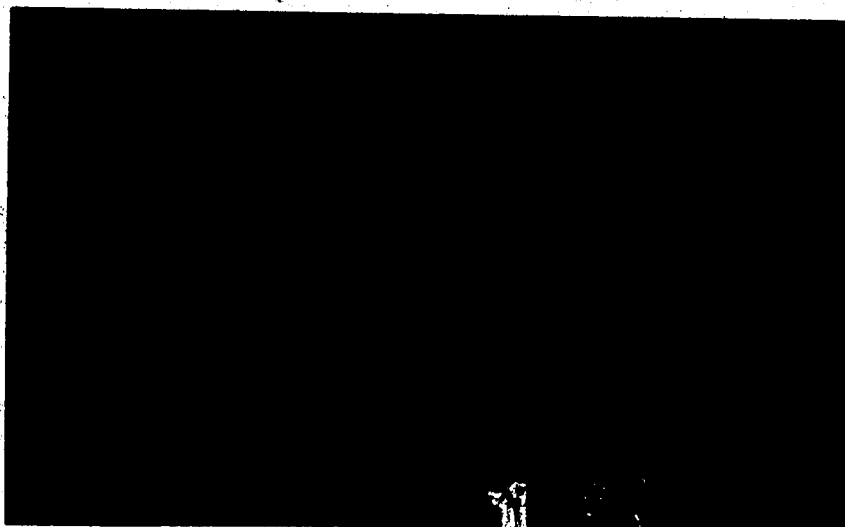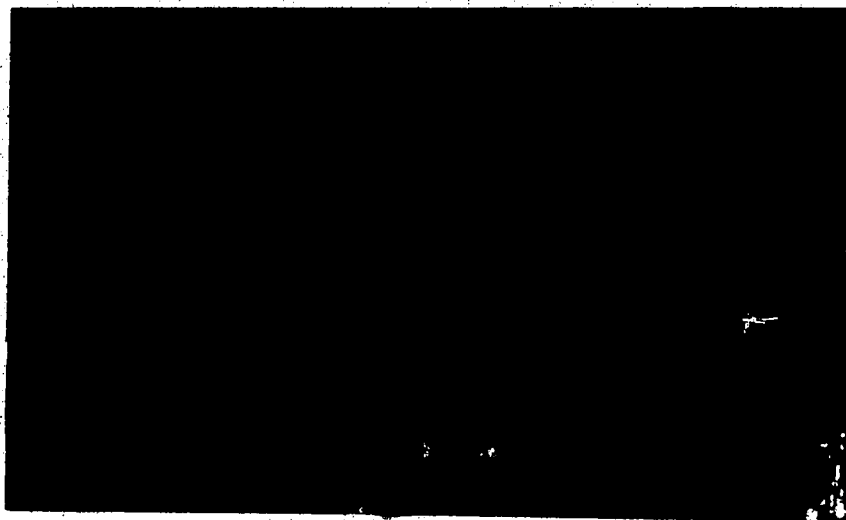

Figure 19. Electrode Negative: Argon - 2% Freon 11, 28 volts, 200 amperes and 800 mm/min (3.8X)
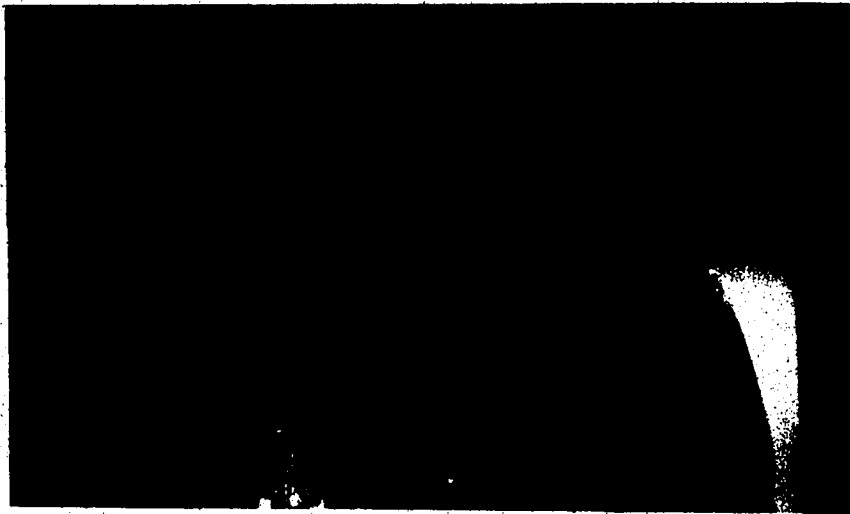
Figure 20. Electrode Negative: Argon - 2% Freon 11, 28 volts, 200
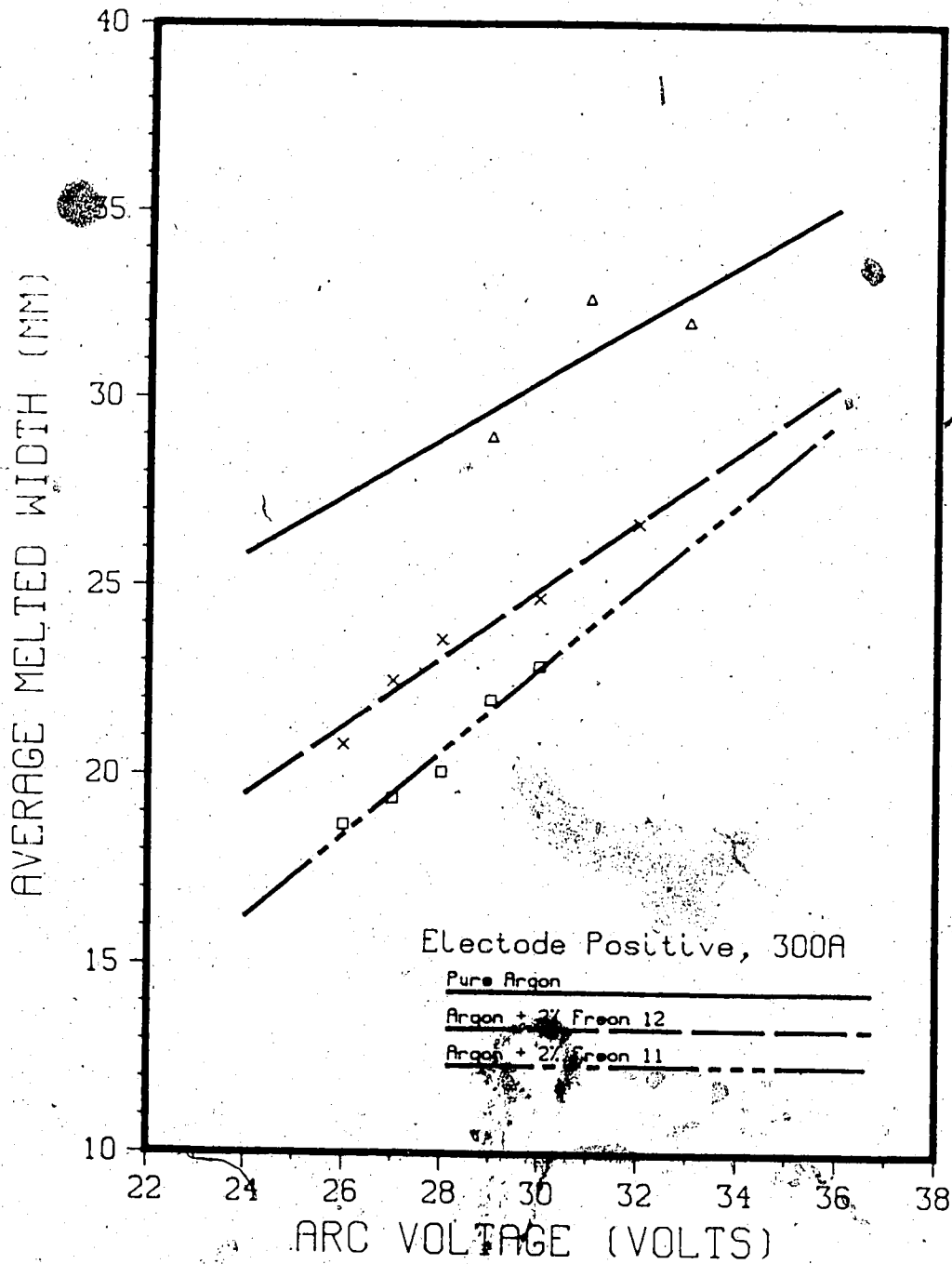amperes and 1000 mm/min (4.2X)

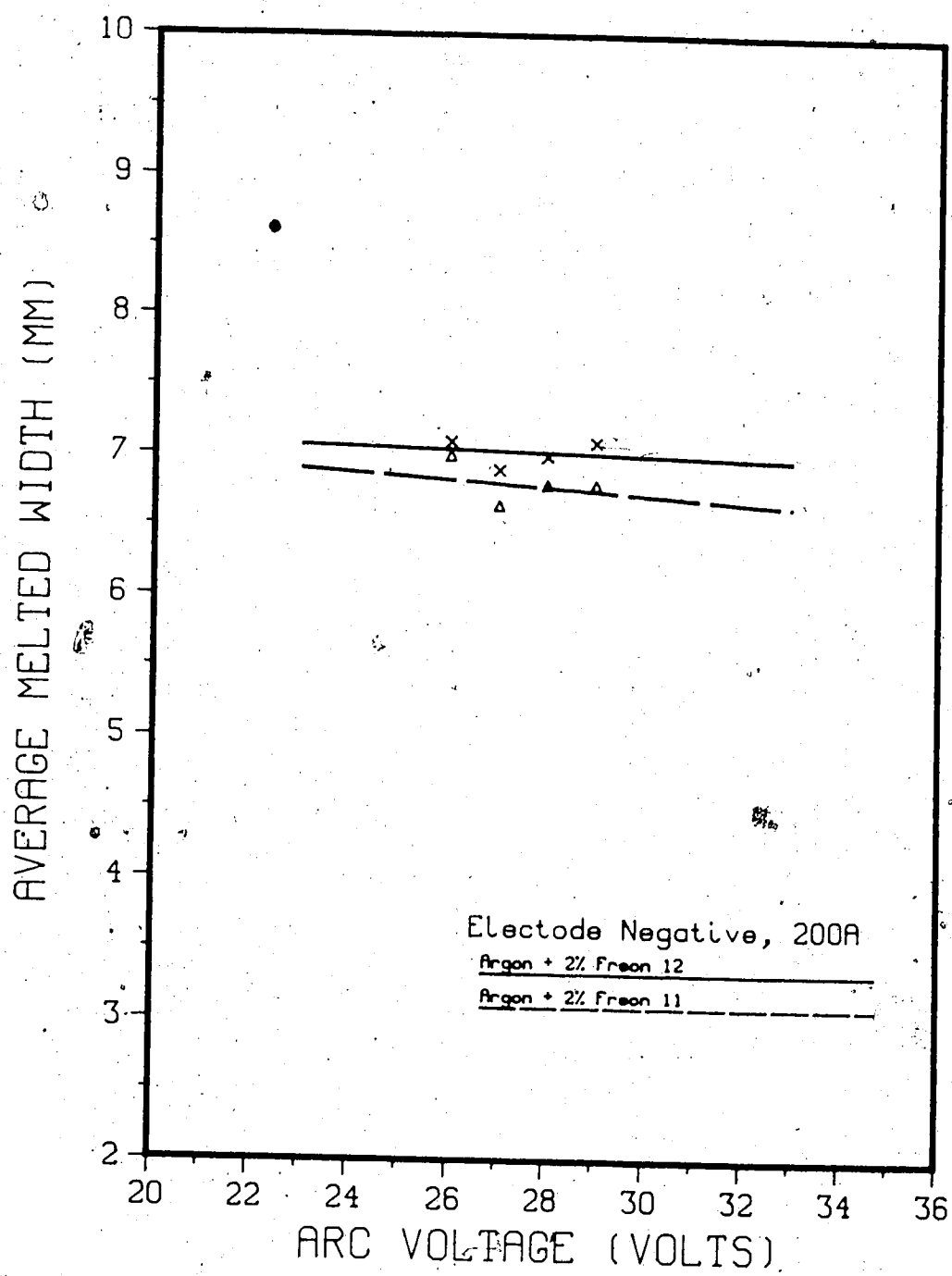Figure 21. Effect of Voltage on Melted Width
with Electrode Positive

Figure 22.   Effect of Voltage on Melted Width
with Electrode Negative

negative: Figures 18 and 23, and electrode positive: Figures 24 to 26) also show that penetration does not decrease as arc voltage increases. Generally when the arc voltage increases, the velocity of the plasma jet decreases due to a decrease in the current density gradient and consequently penetration decreases. However, if the arc length increases significantly due to an increase in arc voltage, the terminal velocity of the droplet at higher arc voltage is sufficiently higher than that at lower arc voltage, thus overcoming the disadvantage of having the lower plasma jet velocity and giving a deeper penetration.

As shown in Figures 21, freon gas additions to the argon produced a narrower weld bead than pure argon and furthermore, 2% freon 11 addition produced a narrower weld bead than 2% freon 12 addition, as shown in Figures 21 and 22. This means that argon - 2% freon 11 gas mixture constricts an arc much better than pure argon or argon - 2% freon 12. As noted by Simonik[26], the halogens constricted the arc column to give increased penetration and decreased fusion width. He also observed that chlorine constricted the arc column more than fluorine and suggested that this was because chlorine has a higher percentage of molecular state at a given high temperature than fluorine.

As described in Section 2.4.3 a molecule tends to capture an electron better than an atom at a high temperature because as soon as an atom becomes a negative ion formed by the addition of an electron at the high arc temperature, it loses the electron due to its unstable high potential energy state. A molecule, however, splits itself to become a negative ion and an atom by capturing the electron and its energy is converted to kinetic energy so that the negative ion and atom become more stable. Therefore, a higher
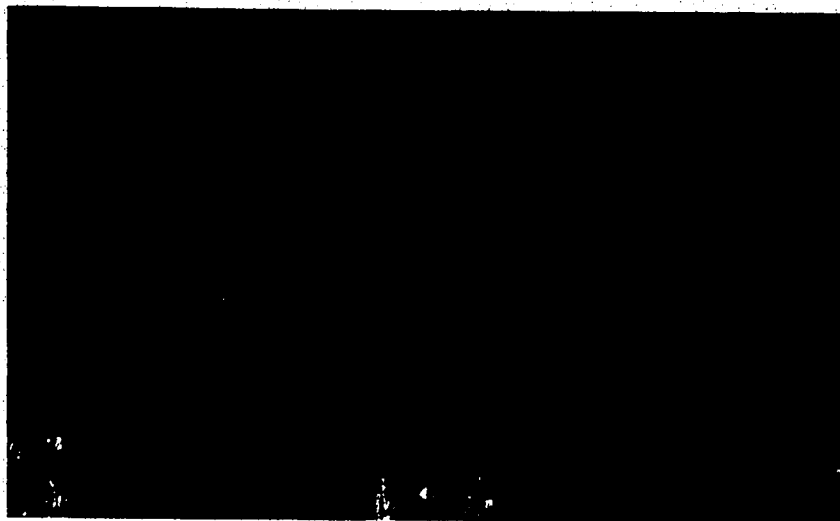
Figure 23. Electrode Negative: Argon - 2% Freon 11, 26 volts, 200 amperes and 400 mm/min (3.9X)
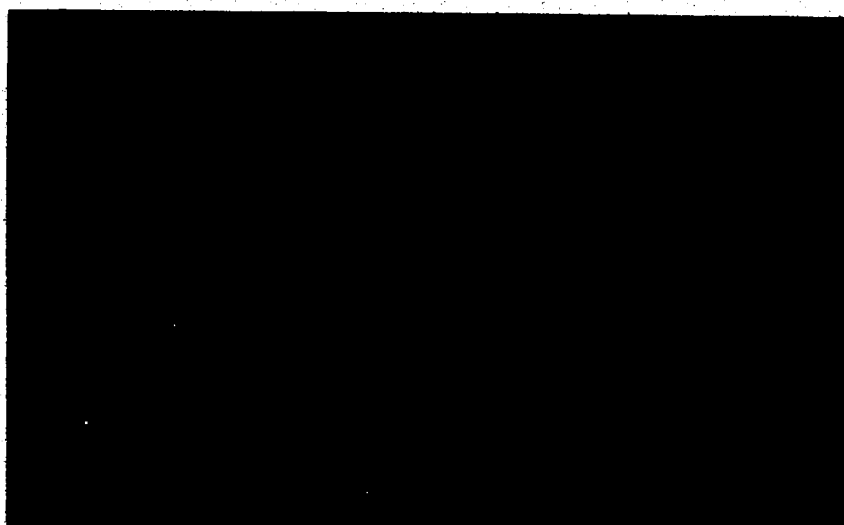

Figure 24. Electrode Positive: Argon - 2% Freon 11, 26 volts, 300 amperes and 240 mm/min (3.4X)
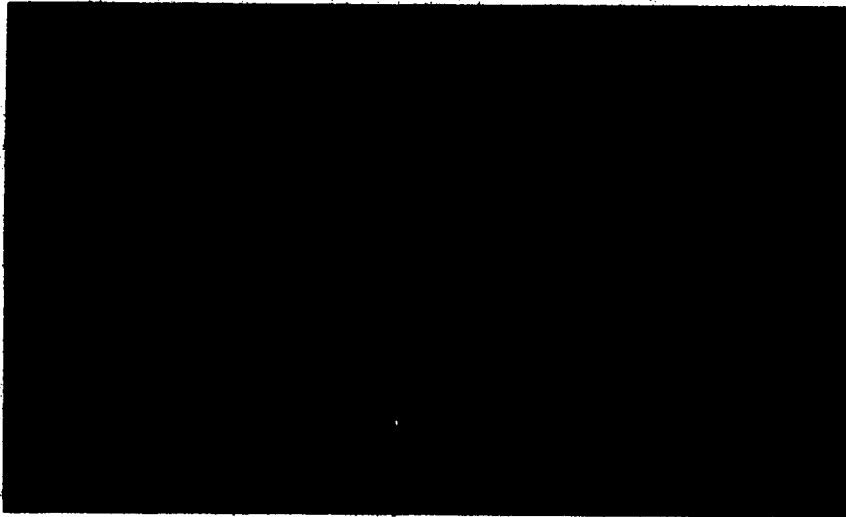
Figure 25. Electrode Positive: Argon - 2% Freon 11, 28 volts, 300 amperes and 240 mm/min (3.4X)
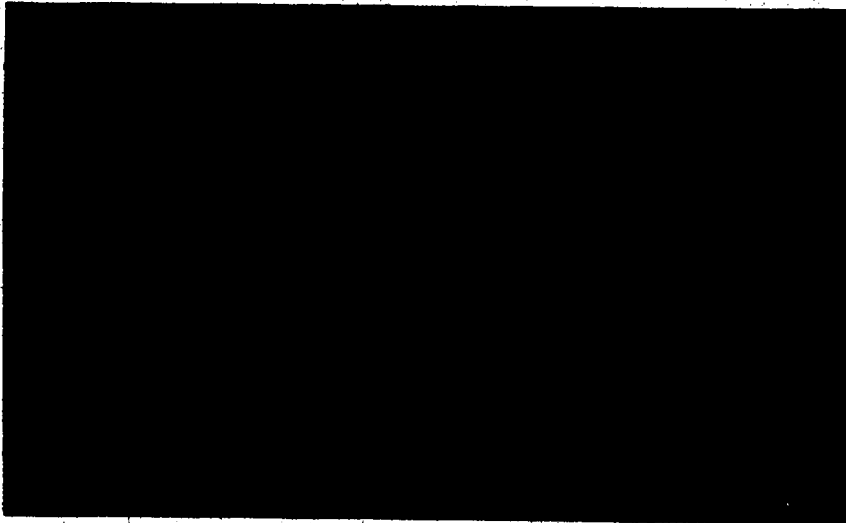
Figure 26. Electrode Positive: Argon - 2% Freon 11, 30 volts, 300 amperes and 240 mm/min (3.4X)

percentage of molecules in the arc column (especially the periphery of the arc column),reduces the number of electrons and lowers the electrical conductivity of the region. This leads to constriction of the arc column. Experiment confirms this theory. Since freon 11 (CCl_3F) contains a higher number of chlorine atoms than freon 12 (CCl_2F_2), argon - 2% freon 11 gas mixture should constrict the arc column more than argon - 2% freon 12 gas mixture. As predicted, argon - 2% freon 11 gas mixture was observed to produce the narrowest weld bead.

4.3 Metal Transfer Characteristics

Metal transfer was studied while welding aluminum by the GMAW process using a high speed video camera at 2000 fps. In the present work, visible arc length, displacement of the drop against time, and frequency of the droplet were evaluated. Pure argon, argon - 2% freon 12 and argon - 2% freon 11 gas mixtures were used as a shielding gas for both D.C. electrode polarities,

4.3.1 Visible Arc Length

As previously mentioned, arc length measurements were electrode-to-plate distances rather than true arc length because craters were formed in the plate under tested conditions. The voltage-arc length curve shows the sum of the anode and cathode potential drop obtained by extrapolating the curve to zero arc length and the plasma potential gradient from the slope of the curve. The results of the tests are shown in Figures 27 and 28 for electrode positive and negative polarity, respectively.

Figure 27. Influence of Arc Length on Voltage
in Electrode Positive
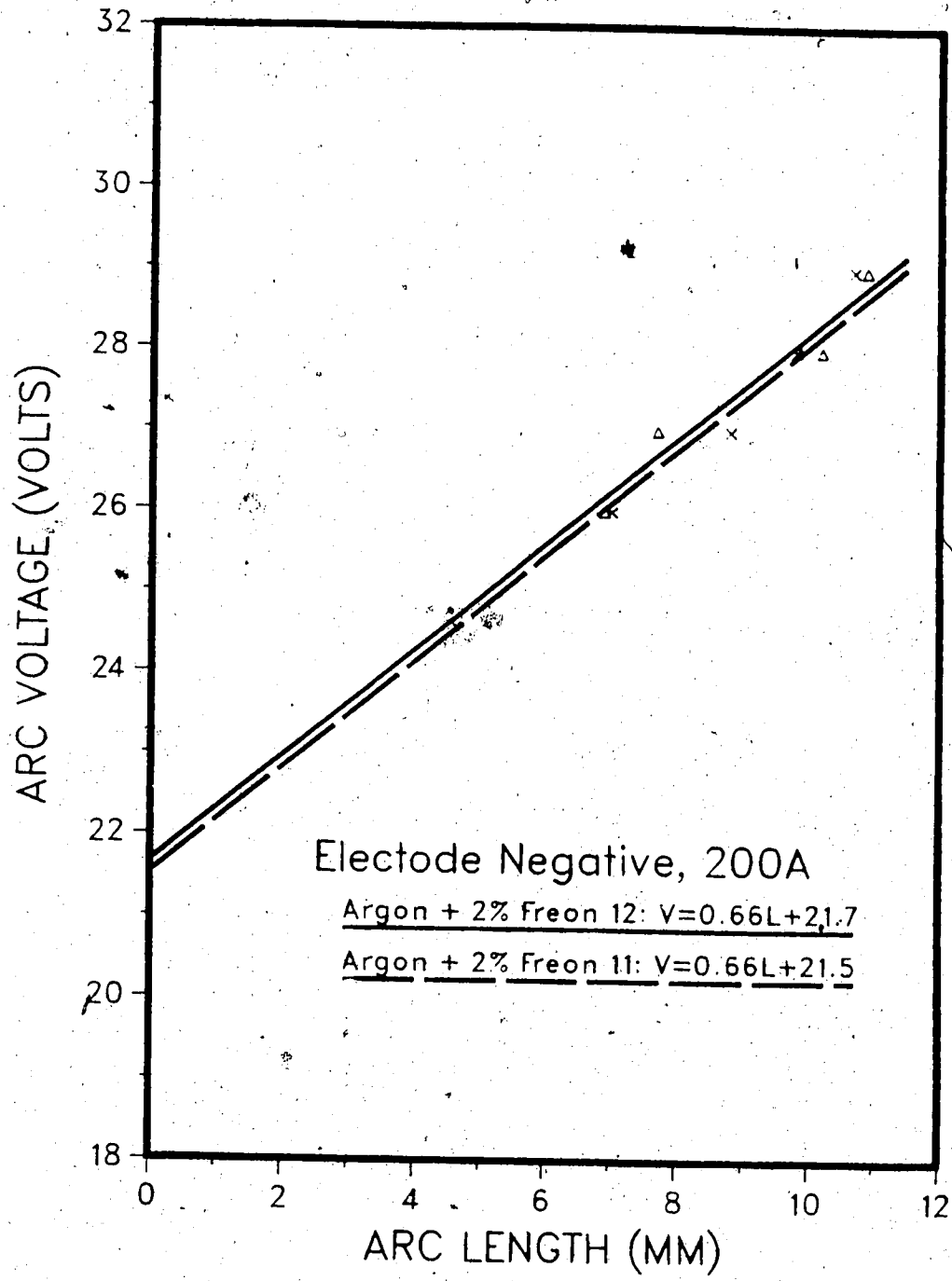
Figure 28 Influence of Arc Length on Voltage
in Electrode Negative

In electrode positive polarity, the voltage gradient for pure argon shielding gas was found to be 0.63 volts/mm, which is same as 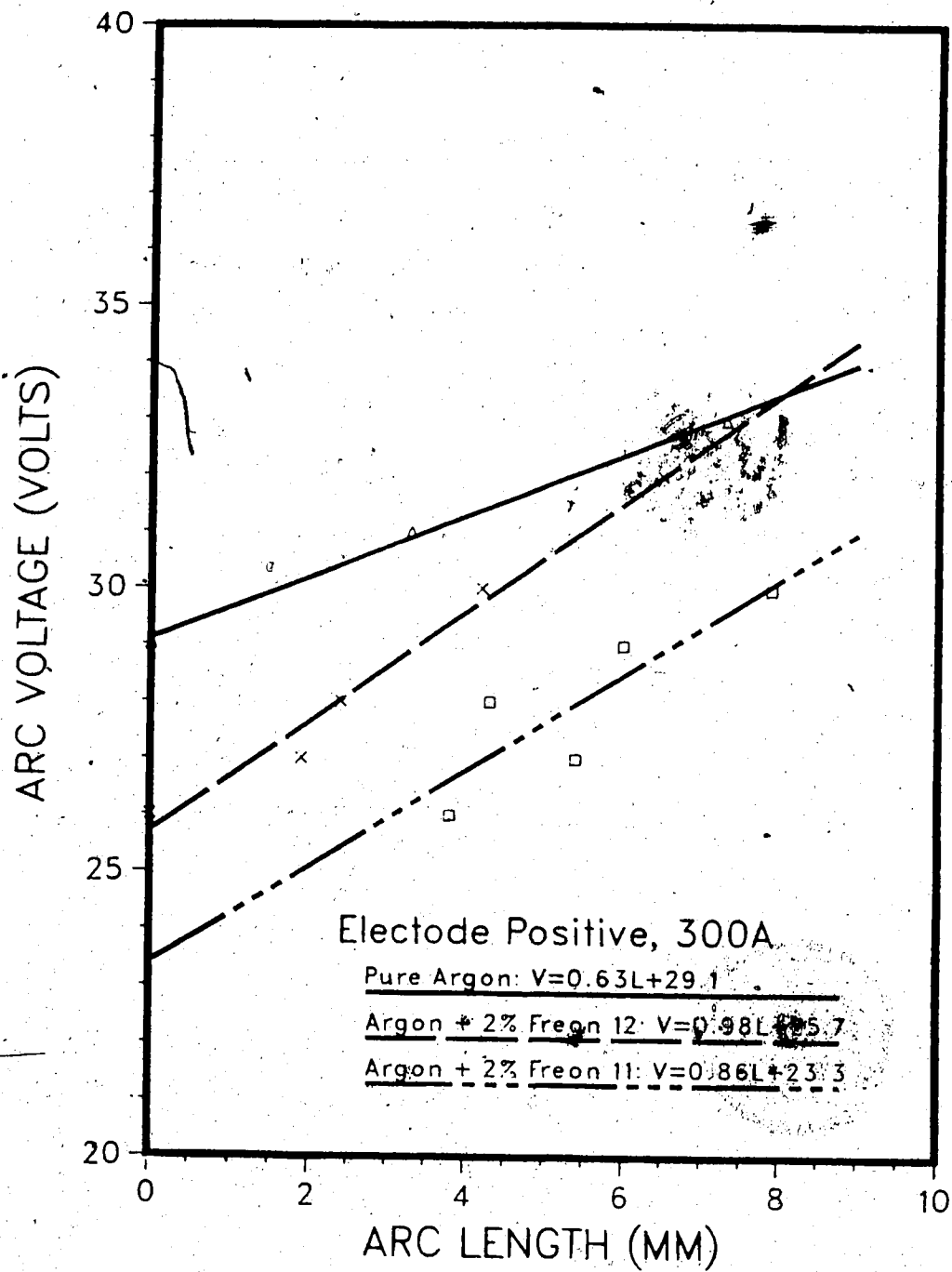Muller's[12] value, while the sum of the anode and cathode drop was 29.1 volts. However, the total electrode voltage drop must be corrected by two subtractions, the total voltage drop due to the wire connections between the work piece to the both terminals and the electrode stickout. These two voltage corrections were found to be approximately 3 volts (2 volts for the wire connections and 1 volt for the electrode stickout). The actual total electrode voltage drop was then 26.1 volts. Other investigators such as Muller el at.[12] and Röll[18] found the total electrode voltage drop to be 21.0 volts at 295 amperes and 1.6 mm diameter electrode and 25.5 volts at 300 amperes and 4.0 mm diameter. However, since the anode potential drop decreases with electrode diameter and rises with current, the experimental value of 26.1 volts is quite acceptable. Voltage gradients for argon - 2% freon 12 (0.98 volts/mm) and argon - 2% freon 11 (0.86 volts/mm) gases were found to be very close to each other but steeper than that of pure argon (0.63 volts/mm). As the voltage gradient gets steeper, the temperature in the arc column increases because the energy dissipated is VI watts per unit length, where V is the voltage gradient along the column and I is the current. Consequently, penetration increases but the cathode potential drop decreases with an increase in arc temperature because the higher arc temperature means more melting in the baseplate and easier production of electrons from the cathode. As shown in Figure 27, the total electrode voltage drops in argon - 2% freon 12 and argon - 2% freon 11 were 25.7 volts and 23.3 volts, respectively, lower than that of pure argon (29.1 volts).

In electrode negative polarity, Figure 28 still shows that both gas mixtures have the same voltage gradient of 0.66 volts/mm and argon - 2% freon 11 has a lower total electrode voltage drop (21.5 volts) than argon - 2% freon 12 (21.7 volts). Since the voltage gradient is lower compared to that in electrode positive polarity, penetration is decreased significantly. Although the cathode potential drop in electrode negative polarity is expected to be higher than that in electrode positive polarity because of the unstable cathode spot area on the electrode, the total electrode voltage drop is lower compared to that in electrode positive polarity. This is because there is enough of a decrease in the anode drop due to the lower current used in electrode negative polarity and the increase in the effective electrode diameter of the anode.

For both electrode polarities, the three gas mixtures can be arranged in the following order of increasing arc length for a given arc voltage: pure argon, argon - 2% freon 12, and argon - 2% freon 11. This can be explained as follows: the total electrode voltage drop was the lowest in the argon - 2% freon 11 gas mixture (Figures 27 and 28). On the basis of these data. the plasma potential drop for a given arc voltage should be highest in the argon - 2% freon 11 gas mixture and therefore this mixture should also have the longest arc length. Furthermore, since argon - 2% freon 11 gas has the highest arc temperature due to its constricted arc column, the electrical conductivity should be increased. This higher electrical conductivity should cause the arc length to get even longer, provided that the effect of 2% freon gas addition to the argon on the overall electrical conductivity is negligible.

4.3.2 The Drop Transfer Rate and Size

The drop transfer rate and droplet size provide a useful means of characterising the nature of metal transfer for the GMAW process. The frequency of the droplet transfer was measured from a T.V. monitor using the time interval between two consecutive drop detachments from the electrode wire, and, knowing the frequency and wire feed rate the diameter of actual size of equivalent sphere for both electrode polarities was calculated. Table 6 shows the summary of the results. For both electrode polarities a voltage increase tends to decrease the frequency. Therefore, it increases the drop diameter within the same shielding gas due to a decrease in the current density gradient. Metal transfer is achieved by a force (pressure drag and skin friction) created by the plasma jet velocity, which depends on the current density gradient, on a molten metal at the end of the electrode. As the plasma jet velocity increases, a higher droplet frequency is achieved. Using pure argon shielding gas and electrode positive polarity at 31 volts and 300 amperes, the frequency and diameter of the droplet were found to be 286 droplets/second and 1.35 mm, respectively. It was shown by Needham and Smith[30] that the frequency and diameter of the droplet were 350 droplets/second and 1.14 mm using parameters which were the same except for arc voltage (22 volts vs. 31 volts). Knowing that a lowering of the arc voltage causes the frequency to decrease and the drop diameter to increase, the results are very close to Needham and Smith's results.

Table 6 also shows how changing the shielding gas affects the frequency and drop diameter. Comparing the three different shielding gas

Table 6.   Summary of Droplet Transfer Rate and Droplet Size for Both
Electrode Polarities

ELECTRODE DIAMETER	CURRENT POLARITY (Amp)	SHIELDING GAS	VOLTAGE (Volts)	FREQUENCY (sec^{-1})	DROP (mm)
Positive	300	Argon	31	286	1.35
			33	277	1.36
		Argon + 2% Freon 12	28	308	1.32
			30	299	1.33
			32	290	1.34
		Argon + 2% Freon 11	28	318	1.30
			29	313	1.31
			30	309	1.32
Negative	200	Argon + 2% Freon 12	27	42.0	2.76
			28	36.0	2.90
		Argon + 2% Freon 11	27	55.8	2.50
			28	50.6	2.58

mixtures for a given voltage and current, argon - 2% freon 11 gas mixture produced the highest frequency and smallest drop diameter. Argon - 2% freon 12 provided a higher frequency and smaller drop diameter than pure argon. On the basis of the above results, it can be concluded that the freon gas additions to the argon shielding gas increase the plasma jet velocity even though the current density gradient for a given voltage decreases due to longer arc length. In particular, the addition of freon 11 provided the highest plasma jet velocity. The elements which affect the plasma jet velocity, and velocity and acceleration of the droplet across the arc, and the calculation of these values will be discussed in the next section.

Table 6 shows that electrode positive polarity gives much better metal transfer than electrode negative polarity. Although the test was carried out at a lower current (200 amperes vs. 300 amperes) on electrode negative polarity, it is doubtful that the difference of 100 amperes would make a such large difference in frequency and drop diameter. For a given current and voltage, electrode negative polarity should provide a shorter arc length because the cathode drop on the electrode tends to be higher than that on the baseplate due to the unstabling of the cathode spot. However, the anode spot area, where electrons are captured, on the baseplate in electrode negative polarity is small because of the lack of an insufficient heat input to break down the large amount of oxides. Since this small anode spot area is much smaller than the cathode spot area on the baseplate in electrode positive polarity, the current density gradient would become much smaller, producing a low plasma jet velocity. Consequently, the frequency of the droplet transfer decreases due to decreasing drag force on a molten metal at

the end of the electrode. It also could be that, in electrode negative polarity, the arc may be established underneath the molten metal at the end of the electrode, instead of surrounding the electrode tip as in electrode positive polarity. In this case, there would not be sufficient force (skin friction and pressure drag) to detach molten droplets from the electrode tip and to propel them across the arc gap to the weld pool. However, this explanation could not be confirmed in this project because the high speed video camera (black and white) at 2000 fps and a xenon backing light were not adequate to provide a clear picture of the arc location with respect to the molten metal.

4.3.3 Velocity and Acceleration of the Droplet

As previously mentioned, the depth of the weld pool is not only influenced by welding current and speed but also by the impact of the droplets of the metal that are detached from the electrode. When metal transfer takes place in a vertically downward direction, the force due to gravity and the plasma jet which acts to detach the drop from the electrode must overcome the restraining force of surface tension of the electrode material. Since the experiments were carried out above the transition current (just over 100 amperes), the force due to gravity is negligible. Therefore, the force exerted on the drop in the plasma jet has a major effect on metal transfer.

The measured velocity and acceleration of the drop for the three different shielding gas mixtures using both electrode polarities are shown in Tables 7 and 8. For purposes of comparison, these drop velocities and accelerations were calculated by measuring the drop displacement after a

Table 7. Summary of Drop Velocity and Acceleration using
Electrode Positive Polarity and 300 Amperes

SHIELDING GAS	VELOCITY[1] (m/sec)	ACCELERATION[2] (m/sec^2)
Pure Argon	2.41	377
Argon + 2% Freon 12	2.45	405
Argon + 2% Freon 11	3.09	900

1) 1.0 msec after drop detachment
2) using $V^2 = U^2 + 2aS$ where $U=2.0$ m/sec

Table 8. Summary of Drop Velocity and Acceleration using
Electrode Negative Polarity and 200 Amperes

SHIELDING GAS	VELOCITY[1] (m/sec)	ACCELERATION[2] (m/sec^2)
Argon + 2% Freon 12	0.755	85.5
Argon + 2% Freon 11	0.834	96.5

1) 4.0 msec after drop detachment
2) using $V^2 = U^2 + 2aS$ where $U=0.228$ m/sec

fixed time interval (i.e., electrode positive: 1.0 msec after drop detachment, electrode negative: 4.0 msec after drop detachment) because the drop velocity increased with time after detachment due to acceleration. Although these values (except for electrode negative polarity) were calculated at different arc voltages, they still can be used for comparison because the overall effect of arc voltage on the velocity and acceleration is negligible compared to the effect of welding current. As illustrated in Table 7 and 8, the shielding gas mixtures can be arranged in the following order of increasing velocity and acceleration effect: pure argon, argon - 2% freon 12 and argon - 2% freon 11. The acceleration was calculated using:

$$V^2 = U^2 + 2aS \qquad (9)$$

where V is the final speed, U is the initial speed, a is the acceleration and S is the distance travelled. Since the experiment was filmed at fps, measuring the initial velocity immediately after detachment was impossible in electrode positive polarity. Instead, an initial velocity of 2.0 m/sec, which was found by Needham et al.[27] using similar welding conditions, was used. Using this initial velocity, Equation 9 gives the acceleration in pure argon of 38.4 gravities which compares well with the average of 40 gravities (with a spread of the order of 25-55) found by Needham et al.[27] using a more precise technique.

This measured acceleration can now be compared with the calculated value using Equation 8. To evaluate Equation 8 for aluminum, the values listed in Table 9 and the calculated value of the axial plasma jet velocity (Equation 6) were used. To estimate the plasma jet velocity, the average arc radius of 3×10^{-3} m, and arc temperature of 15,000 K at 300 amperes

Table 9. Calculated Acceleration of Drops Across the Arc and
the Relevant Variables Used in Calculation

Electrode Polarity   Positive

Current   300 amperes

Mean Temperature   15,000 K

Plasma Jet Velocity   426 m/sec

Drop Radius   0.68 mm

Density of Gas 3.56×10^{-2} kg/m^3

Density of Material 2.0×10^3 kg/m^3

Dynamic Viscosity of Gas 4.2×10^{-4} kg/m sec

Reynolds Number   24.6

Drag Coefficient   2.6

Acceleration   4,640 m/sec^2

were used because the velocity and temperature fall off rapidly in a radial direction. The calculated plasma jet velocity was then found to be 426 m/sec which compares well with Maeker's[32] measurement of 450 m/sec. As a result, the calculated acceleration is estimated to be about 470 gravities at 300 amperes whereas the Needham's[27] theoretical estimate was 250 gravities at 270 amperes. Agreement is reasonably good considering the different welding conditions used. However, note that the calculated acceleration value is not the same as the measured value, partly because the theory assumes that the force remains constant across the arc gap even though there is a significant variation of the acceleration during metal transfer, and also because the values assigned to the variables such as the average arc radius and temperature, dynamic viscosity, and density of gas could be different than the actual values.

It is known that the acceleration of the droplet and plasma jet velocity are largely dependent on the physical properties of the shielding gas which change with temperature (e.g., the freon gas additions to the argon increase the plasma jet velocity, and therefore the velocity and acceleration of the drops are increased accordingly). It is impossible to calculate the plasma jet velocity and acceleration of the drop because the physical properties of freon 11 and 12 are not available, and also freon 11 and 12 start to dissociate at the high temperatures encountered. However, it is possible to compare the physical properties of argon, freon 11 and freon 12 at 100 °C as shown in Table 10. Although there are no data on the physical properties of freons in arc plasma, hopefully comparing these three gases at a lower temperature would permit some assessment of their effects on the plasma jet velocity and acceleration of the drop. Table 10 shows that these

Table 10. The Physical Properties of Argon, Freon 12, and Freon 11

	Density (kg/m³)	Dynamic Viscosity (kg/m sec)
Argon	1.289	2.74×10^{-5}
Freon 12	3.393	1.45×10^{-5}
Freon 11	4.500	1.35×10^{-5}

* All data is based on Pressure = 0.1 Mpa and Temperature = 100 °C

gases can be arranged in the following order of increasing density or decreasing dynamic viscosity: argon, freon 12 and freon 11. Knowing that the plasma jet velocity is inversely proportional to the dynamic viscosity (Equation 6) and the acceleration is proportional to the density and square of the plasma jet velocity (Equation 8), it can be concluded that the argon-freon 11 gas mixture should give the highest plasma jet velocity for a given temperature regardless of electrode polarity. This explains the observation that the acceleration of the droplet in the argon - 2% freon 11 gas mixture was found to be the highest, as shown in Tables 7 and 8.

The overall experimental results showed that the halogens increased penetration and decreased fusion width. This implies that halogens constricted the arc column, and furthermore that among the halogen atoms chlorine constricted the arc column more than fluorine. Therefore, the argon - 2% freon 11 would be expecte████████████ the arc column more than argon - 2% freon 12 or pure argon to produce the narrowest weld bead because freon 11 contains a higher number of chlorine atoms. However, constriction of the arc column due to the freon additions could not be observed on a T.V. monitor.

The total electrode voltage drop was the lowest in the argon - 2% freon 11 gas mixture with both polarities. As a result, the plasma potential drop in this gas mixture should be the largest for a given arc voltage, and therefore should also have the largest arc length. Furthermore, since argon - 2% freon 11 gas has the highest arc temperature due to its constricted arc column, the electrical conductivity would increase allowing the arc length to get even longer, as observed.

For both polarities a voltage increase within the same shielding gas tends to decrease the droplet transfer frequency because of a decrease in the current density gradient. However, electrode positive polarity gives a much higher droplet transfer frequency than electrode negative polarity. This is because the current density gradient is much lower in electrode negative polarity due to the small anode spot area on the baseplate.

The droplet transfer frequency and penetration are largely influenced by the plasma jet velocity which itself is governed by the current density gradient and physical properties of the gas. Although argon - 2% freon 11 gas gave the smallest current density gradient due to it having the longest arc length and narrowest weld bead for a given arc voltage and current, it produced the highest plasma jet velocity with the best penetration and highest droplet transfer frequency among the three shielding gases tested. There are two reasons that can explain these contradicting results. Firstly, argon - 2% freon 11 gas has the better physical properties (i.e., a lower dynamic viscosity and higher density) thus allowing a higher plasma jet velocity. Secondly, since it constricts an arc more than other gases, it has the smallest cross section area through which a given volume of the plasma jet can pass, increasing the plasma jet velocity significantly. This experiment, therefore, clearly showed that adding freon gas containing a higher number of chlorine atoms to the argon as a shielding gas provided better metal transfer.

4.4 Mechanical Properties of Weld Metals

Once the effects of arc voltage, current and welding speed on weld profile, and metal transfer characteristics were studied, the mechanical

properties of weld metals using pure argon and argon - 2% freon 11 gas mixtures with electrode positive polarity were assessed. First, two types of single-V grooves (Figure 7) were tested and the results obtained using the same welding conditions are shown in Figures 29A and 29B. The deeper groove shows a crown almost identical to that of the shallower groove but with deeper penetration. For this reason, all the groove welding and mechanical testing was done using the deeper groove. As with beads on plate testing, current and welding speed were altered to see the effects on weld profile. Figures through 33 reveal that the use of 26 volts, 300 amperes and 240 mm gave the best weld profile. Under the same conditions, argon-1% freon 11 gas mixture, as shown in Figure 34, gave an increased fusion width (due to the longer arc) but reduced stability. Pure argon (Figure 35) produced still less penetration and fusion width compared with the argon - 2% freon 11 gas mixture.

Table 11 summarizes the mechanical properties of weld metals. A tensile test on 5086 baseplate showed that the material had an ultimate tensile strength of 308 MPa, an area reduction of 33.4% and elongation in 5.1 mm of 19%. Other tensile test results on welded specimens were compared to these values. The ultimate tensile strength and elongation values for both transverse tensile specimens, with reinforcement removed, from pure argon and argon - 2% freon 11 were lower than the values from the baseplate but the specimen from argon - 2% freon 11 showed higher values than the specimen from pure argon. The all weld metal machined tensile specimen from argon - 2% freon 11 showed almost the same ultimate tensile strength with a higher elongation value compared to the transverse tensile specimen with reinforcement removed. Both small and
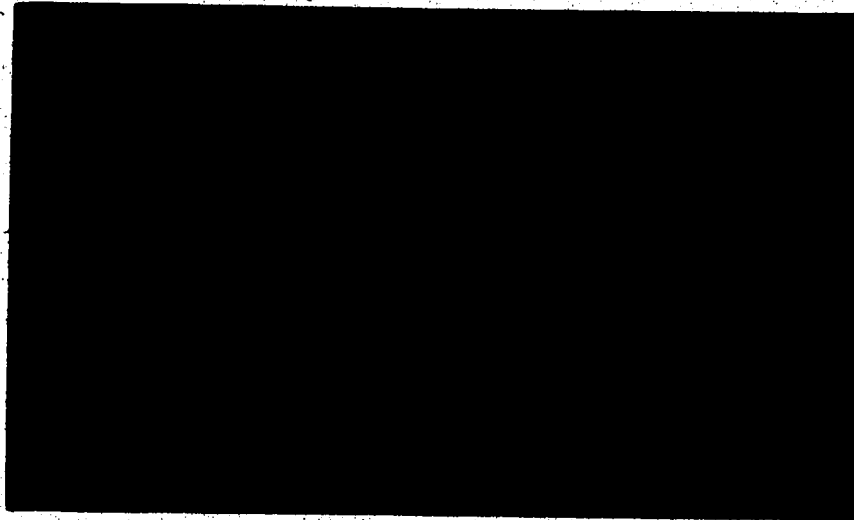
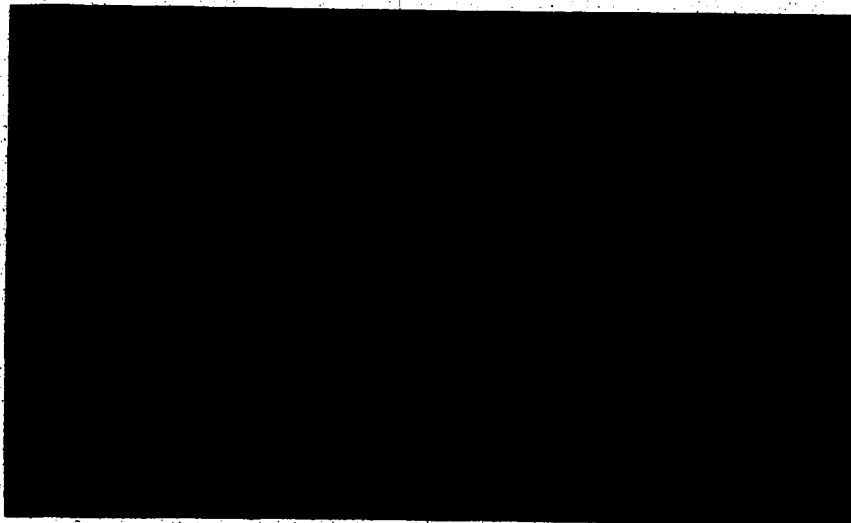Figure 29A. Electrode Positive: Type 1 Edge Preparation (2.9X)

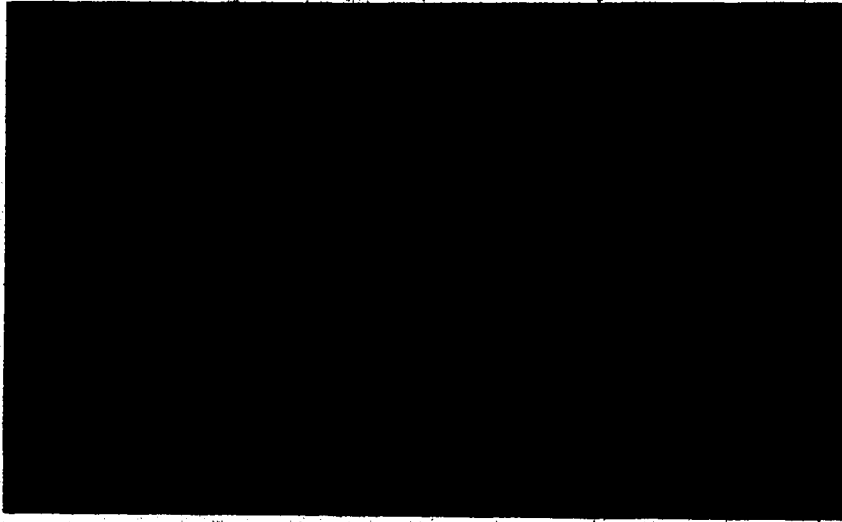Figure 29B. Electrode Positive: Type 2 Edge Preparation (3.2X)

Figure 30. Electrode Positive: Argon - 2% Freon 11, 26 volts, 325 amperes and 300 mm/min (3.1X)
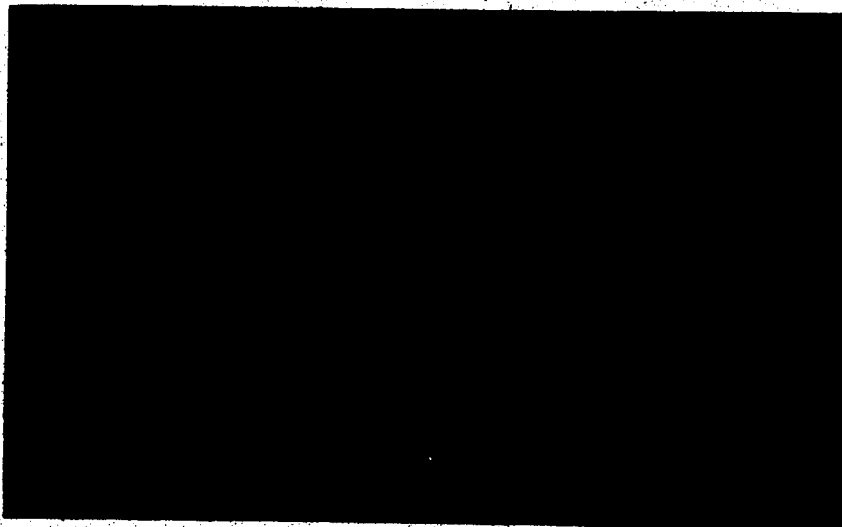

Figure 31. Electrode Positive: Argon - 2% Freon 11, 26 volts, 300 amperes and 300 mm/min (3.1X)
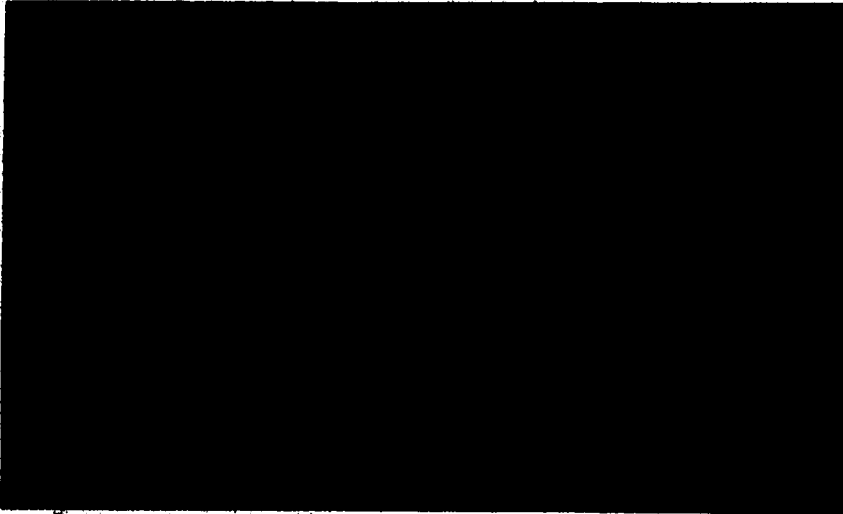
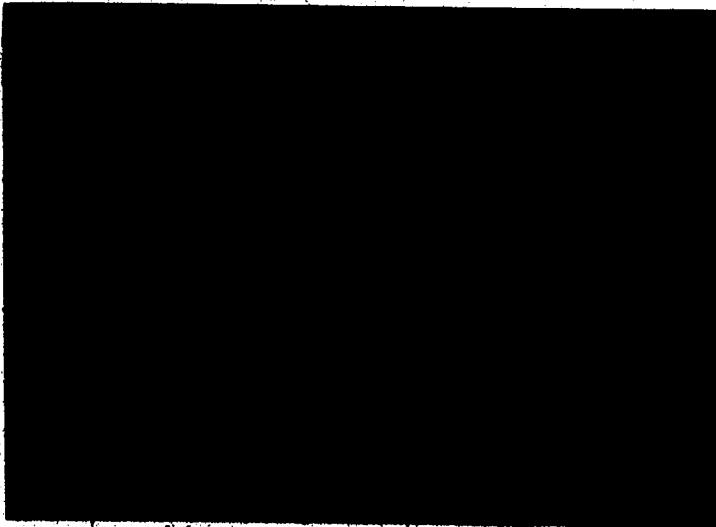Figure 32. Electrode Positive: Argon - 2% Freon 11, 26 volts, 300 amperes and 200 mm/min (3.0X)

Figure 33. Electrode Positive: Argon - 2% Freon 11, 26 volts, 300 amperes and 240 mm/min (2.4X)
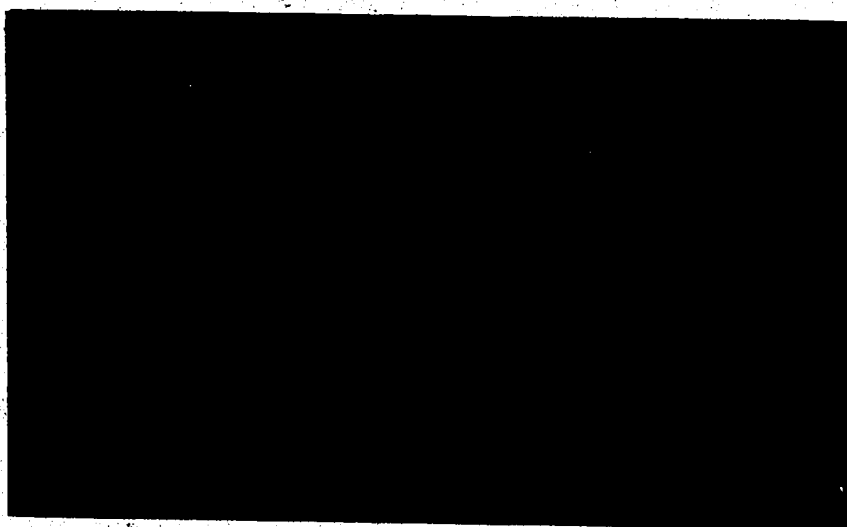
Figure 34. Electrode Positive: Argon - 1% Freon 11, 26 volts, 300 amperes and 240 mm/min (3.1X)
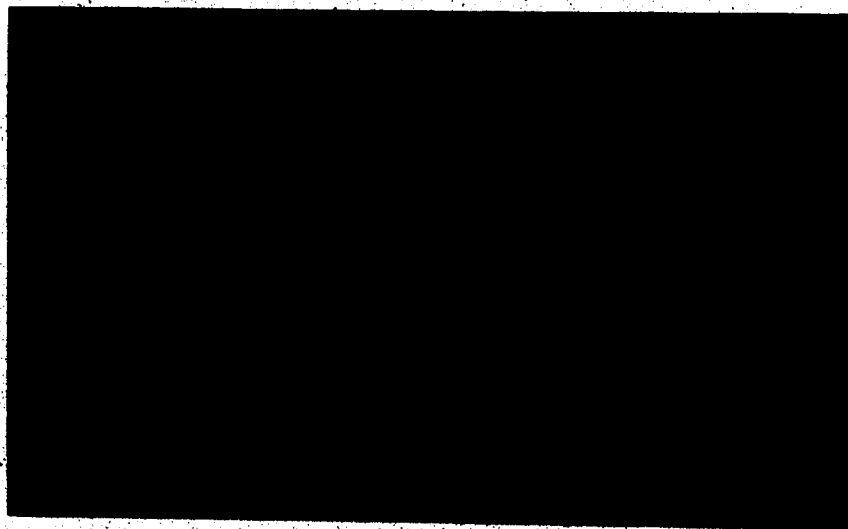
Figure 35. Electrode Positive: Pure Argon, 26 volts, 250 amperes and 240 mm/min (2.9X)

Table 11. Summary of Tensile Test Data

SPECIMEN	UTS (MPa)	ELONGATION (%)*	ELONGATION (%)**	AREA REDUCTON (%)
5086 Baseplate	308.0	19	-	33.4
Pure Argon Transverse with Reinforcement Removed	250.8	16	27	29.0
Argon - 2% Freon 11 All Weld Metal Machined	256.3	25	-	33.5
Argon - 2% Freon 11 Transverse with Reinforcement Removed	267.3	18	35	39.0
Argon - 2% Freon 11 Transverse with Reinforcement	315.6	19	18	26.0
Argon - 2% Freon 11 Transverse with Reinforcement Large Specimen	290.1	22	22	20.0

* 2.0in Gauge Length

** 0.75in Gauge Length in Weld Metal

large transverse tensile specimens with reinforcement from the argon - 2% freon 11 gas mixture gave almost the same values as the baseplate. Both specimens failed at the HAZ (heat affected zone). On the whole, it can be seen that the ultimate tensile strength and elongation of the specimen from argon - 2% freon 11 were better than the specimen from pure argon.

5. Conclusions

It has been shown previously that the additions of freon gases containing carbon and the halogen atoms fluorine, bromine and chlorine, to argon provides an effective means of improving arc stability and weld bead characteristics (e.g. penetration) for welding aluminum alloys on both D.C. electrode negative and positive polarity with the GMAW process. Furthermore, among the halogen atoms, chlorine was shown to provide the most marked improvements in arc characteristics. However, prior to this work, nothing had been published on the use of freon 11 (CCl_3F), containing higher numbers of chlorine atoms than other freon gases, as an addition to argon shielding gas.

In this present work, three shielding gas mixtures were tested and compared: pure argon, argon - 2% freon 12 and argon - 2% freon 11. The following conclusions are the findings of this research:

1. By adding 2% of freon 11 to the argon, the arc becomes very stable resulting in remarkable weld profile regularity and deeper penetration on both electrode polarities than pure argon or argon - 2% freon 12.

2. An increase in welding current increases the depth and width of the weld penetration, the deposition rate, and the size of the weld bead when all other welding variables are held constant.

3. Using bead-on-plate tests, the optimum welding speed for electrode positive polarity in argon - 2% freon 11 gas is 400 mm/min at 26 volts and 325 amperes.

4. A voltage increase tends to increase the fusion width in electrode positive polarity, but the fusion width becomes relatively constant regardless of arc voltage in electrode negative polarity due to an insufficient heat input on the baseplate (anode).

5. Argon - 2% freon 11 gas produces the narrowest weld bead on both electrode polarities. This is believed to occur because the halogen atoms, especially chlorine, tend to constrict the arc column by reducing the number of electrons at the periphery of the arc column.

6. The addition of freon gases to argon provides a steeper voltage gradient than pure argon, and therefore the arc temperature increases. This increase in the arc temperature is responsible for the better penetration observed.

7. Argon - 2% ████████ produces the lowest total electrode voltage drop, ██████████ the longest arc length for a given arc voltage ██████████ polarities.

8. With ██████████ a voltage increase tends to increase arc length ██████████ droplet transfer frequency. This is caused by a decrease ████ the current density gradient .

9. Electrode positive polarity gives much better metal transfer than electrode negative polarity. It is suggested that this is caused by the higher plasma jet velocity.

10. Argon - 2% freon 11 gas produces the best penetration and highest velocity and acceleration of the droplet even though it has the lowest current density gradient for a given arc voltage.

11. The three shielding gas mixtures can be arranged in order of increasing plasma jet velocity effect: pure argon, argon - 2% freon 12 and argon - 2% freon 11.

12. Since the operating current is well above the transition current (about 100 amperes for 1.6 mm diameter aluminum electrode), the velocity and acceleration of the drop is largely governed by the plasma jet velocity. These three shielding-gas mixtures, therefore, can be arranged according to increase of the velocity and acceleration of the drop effect in the same order as above.

13. The ultimate tensile strength and elongation values for a transverse tensile specimen, with reinforcement removed, from the argon - 2% freon 11 gas mixture are slightly lower than the values from the baseplate but higher than the values from welds made in pure argon. However, a transverse tensile specimen with reinforcement gives almost the same values as the baseplate. Therefore, the use of freons in the shielding gas does not impair the mechanical properties of the welded joint.

6. Recommendations for Future Work

Tests have been conducted to evaluate the effect of argon-freon shielding gas mixtures on GMAW of aluminum using both electrode polarities. Results have indicated that an adding 2% of freon 11 to the argon improves arc stability and weld bead characteristics on both electrode polarities. The following suggestions, however, are recommended for topics of further research:

1. An attempt should made to design a probe mechanism which measures the electrical conductivity of an arc column cross section. This would help to determine how much the freon additions to the argon as a shielding gas affect constriction of the arc column by lowering the conductivity of the periphery of the arc column.

2. An attempt should also be made to develop a probe capable of measuring the temperature of an arc column cross section. The temperature profile of the arc column cross section would be then used in conjunction with the electrical conductivity of the arc column to assess the overall effects of the freon additions to the argon in more detail (e.g. the physical properties of the gases such as viscosity and density in arc plasma).

3. A more precise technique should be used to analyse metal transfer in welding arc. A high speed video camera using 2000 fps and a black & white film was not fast enough to measure the initial velocity of the droplet and not clear enough to provide a distinct picture of the arc column on a T.V. screen.

References

1. Norrish, J., "High Deposition MIG Welding With Electrode Negative Polarity", Paper 16, Third Conference on 'Advances in Welding Processes', The Welding Institute Harrogate, 1974.

2. Collins, F.R., "Porosity in Aluminum Alloy Welds", Weld. J., Vol. 37 (6), pp 589-593, 1958.

3. Matchett, R.L., and Frankhouser, W.L., "Halogen Additions to Inert Atmosphere Weld Chambers", AEC Report, Contract AT-11-1 GEN-14, May 1960.

4. Lundin, C.D., and Ruprecht, W.J., "The Effect of Shielding Gas Additions on the Penetration Characteristics of Plasma Arc Welds", Weld. J., Vol. 56 (1), pp 1s-7s, 1977.

5. Patchett, B.M., "MIG Welding of Aluminum with an Argon-Chlorine Mixture", Metal Construction, Vol. 10, No. 10, pp 484-485, 1978.

6. Bicknell, A.C., and Patchett, B.M., "GMA Welding of Aluminum with Argon/Freon Shielding Gas Mixtures", Weld. J., Vol. 64 (5), p 21, 1985.

7. Lancaster, J.F., "Energy Distribution in Argon Shielded Welding Arcs", Brit. Weld. J., Brit. Weld. J., Vol. 1, pp 412-426, 1954.

8. Morris, A.D., and Gore, W.C., "Analysis of the Direct Current Arc", Weld. J., Vol. 35, pp 137s-144s, 1956.

9. Olsen, H.N., "Temperature Measurements in High Current Arc Plasmas", Amer. Phys. Soc. Bulletin, P81, January 29th, 1957.

10. Verchenk, V.R., "Static Arc Characteristics in Gas Shield Welding with Fusion Electrodes", Avtomat. Svarka, No. 8, pp 75-78, August 1958.

11. Wooding, W.H., "The Inert Gas Shielded Metal Arc Welding Process", Weld. J., Vol. 32 (4,5), pp 299-312, pp 407-423,1953.

12. Muller, A., Green, W.J., and Rothschild, G.R., "Characteristics of Inert Gas Shielded Metal Arcs", Weld. J., Vol. 30 (8), pp 717-727, 1951.

13. Kiyohara, M., Okada, O., Wakino, Y., and Yamamoto, H., "On the Stabilization of GMA Welding of Aluminum", Weld. J., Vol. 56 (3), pp 20-28, 1977.

14. Conrady, H. von., "Spannungsverteilung im Schweisslichtbogen", Elektroschwg., Vol. 8, pp 101-106, pp 125-128, 1937.

15. Mason, R.C., "Probe Measurements on High Pressure Arcs", Phys. Rev., Vol. 51, pp 28-42, 1937.

16. Frett, G.H., "Cathode Drop of an Arc", Weld. J., Vol. 21 (1), Research Suppl., 27s-29s, 1942.

17. Betz, P.L., and Karrer, S., " A Characteristic of the Copper Arc During the Formative Period", J. App. Phys., Vol. 8, pp 845-848, 1937.

18. Röll, W., "Der Spannungsfall im Schweisslichtbogen", Thesis, Berlin, 1962.

19. Kesaev, I.G., "Laws Governing the Cathode Drop and the Threshold Currents in an Arc Discharge on Pure Metals", Soviet Physics - Technical Physics, Vol. 9, No. 8, 1962.

20. Tomlinson, J.E., and Slater, D., "Automatic Welding of Aluminum Plate", Paper presented at the Public Session of the Vienna Assembly of the IIW, June 1958.

21. Rockefeller, M.E., "Fundamentals of Inert Gas Shielding Arc Welding", Weld. J., Vol. 30 (8), pp 711-716, 1951.

22. Rockefeller, M.E., "Inert Gas Shielded Arc Consumable Electrode Welding", Ibid., Vol. 31 (7), pp 575-586, 1952.

23. Cunningham, J.W., and Cook, H.C., "A Comparison of Shielding Mixtures for Gas Shielded Arc Welding", Ibid., Vol. 32 (9), pp 834-841, 1953.

24. Dowd, J.D., "Inert Shielding Gases for Welding Aluminum", Ibid., Vol. 36 (4), Research Suppl., pp 207s-211s, 1956.

25. Hilton, D.E., "He/Ar gas mixtures prove more economic than Ar for Al welds", Welding and Metal Fabrication, Vol. 50 (5), pp 232-240, June 1982.

26. Simonik, et al., "The Influence of Various Halides on Penetration in the Argon Arc Welding of Titanium Alloys", Svar. Proiz., No. 3, pp 52-53, 1974.

27. Needham, J.C., Cooksey, C.I., and Milner, D.R., "The Transfer of Metal in Inert Gas Shielded Arc Welding", Brit. Weld. J., Vol. 7, pp 101-114, 1960.

28. Nishiguchi, K., and Matsunawa, A., "Gas Metal Arc Welding in High Pressure Atmospheres", IIW. Document 212-371-76.

29. Cooksey, C.J., and Milner, D.R., "Metal Transfer in Gas Shielded Arc Welding", Proceedings of Conference on Physics of the Welding Arc, London, p 123, 1962.

30. Needham, J.C., and Smith, A.A., "Arc and Bead Characteristics of Aluminum Self-adjusting Arc", Brit. Weld. J., Vol. 5 (2), pp 66-76, 1958.

31. Metals Handbook: Desk Edtion, American Society for Metals, Metals Park, Ohio, 1985.

32. Maeker, H., "Plasma Streaming in Arcs as a Results of Self-induced Magnetic Compression", Z. für Physik, Vol. 141, p. 198, 1955.